

UCSF

UC San Francisco Previously Published Works

Title

The lysine methyltransferase SMYD5 amplifies HIV-1 transcription and is post-transcriptionally upregulated by Tat and USP11

Permalink

<https://escholarship.org/uc/item/2g6347mp>

Journal

Cell Reports, 42(3)

ISSN

2639-1856

Authors

Boehm, Daniela

Lam, Victor

Schnolzer, Martina

et al.

Publication Date

2023-03-01

DOI

10.1016/j.celrep.2023.112234

Peer reviewed



Published in final edited form as:

Cell Rep. 2023 March 28; 42(3): 112234. doi:10.1016/j.celrep.2023.112234.

## The lysine methyltransferase SMYD5 amplifies HIV-1 transcription and is post-transcriptionally upregulated by Tat and USP11

Daniela Boehm<sup>1,2</sup>, Victor Lam<sup>4</sup>, Martina Schnolzer<sup>5</sup>, Melanie Ott<sup>1,2,3,6,\*</sup>

<sup>1</sup>Gladstone Institute of Virology, University of California, San Francisco, San Francisco, CA 94158, USA

<sup>2</sup>Department of Medicine, University of California, San Francisco, San Francisco, CA 94143, USA

<sup>3</sup>Chan Zuckerberg Biohub, San Francisco, CA 94158, USA

<sup>4</sup>Tetrad Graduate Program, Department of Pharmaceutical Chemistry, University of California, San Francisco, San Francisco, CA 94158, USA

<sup>5</sup>Functional Proteome Analysis, German Cancer Research Center (DKFZ), 69120 Heidelberg, Germany

<sup>6</sup>Lead contact

### SUMMARY

A successful HIV-1 cure strategy may require enhancing HIV-1 latency to silence HIV-1 transcription. Modulators of gene expression show promise as latency-promoting agents *in vitro* and *in vivo*. Here, we identify Su(var)3–9, enhancer-of-zeste, and trithorax (SET) and myeloid, Nery, and DEAF-1 (MYND) domain-containing protein 5 (SMYD5) as a host factor required for HIV-1 transcription. SMYD5 is expressed in CD4<sup>+</sup> T cells and activates the HIV-1 promoter with or without the viral Tat protein, while knockdown of SMYD5 decreases HIV-1 transcription in cell lines and primary T cells. SMYD5 associates *in vivo* with the HIV-1 promoter and binds the HIV trans-activation response (TAR) element RNA and Tat. Tat is methylated by SMYD5 *in vitro*, and in cells expressing Tat, SMYD5 protein levels are increased. The latter requires expression of the Tat cofactor and ubiquitin-specific peptidase 11 (USP11). We propose that SMYD5 is a host activator of HIV-1 transcription stabilized by Tat and USP11 and, together with USP11, a possible target for latency-promoting therapy.

This is an open access article under the CC BY-NC-ND license (<http://creativecommons.org/licenses/by-nc-nd/4.0/>).

\*Correspondence: [mott@gladstone.ucsf.edu](mailto:mott@gladstone.ucsf.edu).

#### AUTHOR CONTRIBUTIONS

D.B. and M.O. designed and guided the study. D.B. designed, performed, and analyzed biochemical experiments. V.L. tagged and cloned SMYD5-WT into the EF-1 $\alpha$ -pBOS vector. M.S. provided recombinant Tat proteins. M.O. supervised the experiments and helped with data interpretation. M.O. and D.B. secured funding. The manuscript was written by D.B. and M.O.

#### DECLARATION OF INTERESTS

The authors declare no competing interests.

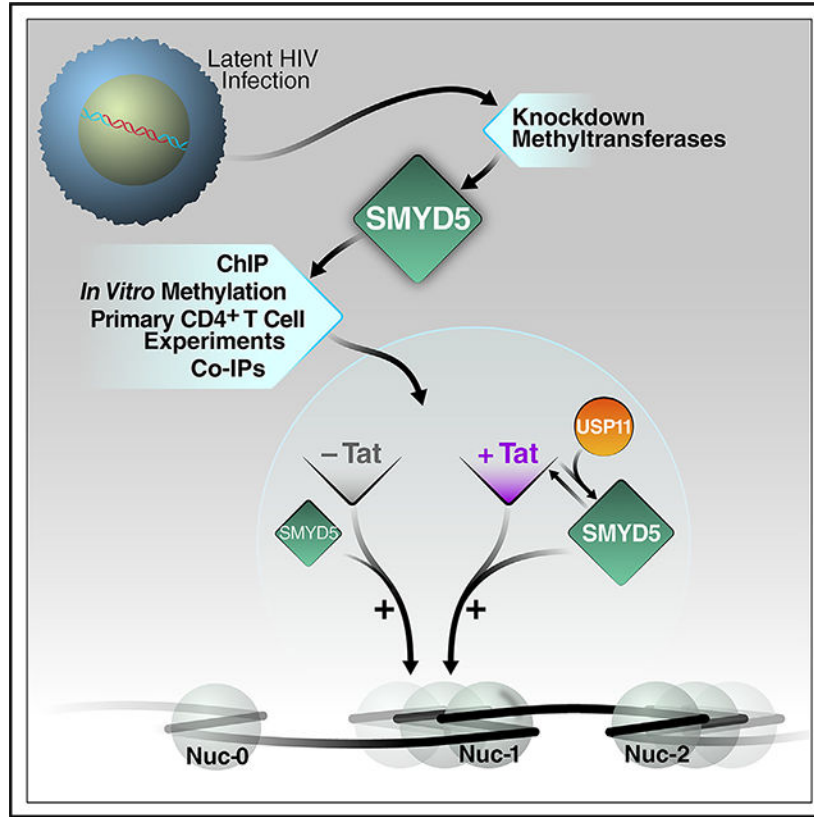
#### SUPPLEMENTAL INFORMATION

Supplemental information can be found online at <https://doi.org/10.1016/j.celrep.2023.112234>.

### In brief

The data presented here connect the lysine methyltransferase SMYD5 with HIV-1 transcription. Boehm et al. propose that SMYD5 is a host coactivator of HIV-1 transcription by itself but is also stabilized by the viral Tat protein and the ubiquitin-specific peptidase 11 (USP11) and a possible target for latency-promoting therapy.

### Graphical Abstract



### INTRODUCTION

Epigenetic regulation by methylation and acetylation of DNA and methylation, acetylation, and ubiquitination of histone and non-histone proteins play an important role in HIV transcription and are targets in preclinical efforts to tackle HIV-1 latency, a major hurdle to curing HIV-1 infection. HIV-1 latency is established after viral DNA integrates into the host chromatin.<sup>1</sup> When integrated, proviral cDNA is transcriptionally silenced and becomes subject to regulation by host chromatin-modifying enzymes, including lysine methyltransferases (KMTs) and demethylases.<sup>2-4</sup> These epigenetic modulators are targets for latency-reversing or latency-promoting therapeutic strategies where either transcriptional corepressors or coactivators are inhibited, respectively, to eradicate latent HIV-1. Although many transcriptional activators for HIV-1 have been identified, they have so far failed to significantly reduce the size and impact of latent HIV-1 reservoirs.

A critical virus-encoded regulator of HIV-1 transcription is the Tat protein. Tat binds to an RNA stem-loop structure called HIV trans-activation response (TAR) element at the 5' end of all nascent viral transcripts and recruits the positive transcription elongation factor P-TEFb, composed of Cyclin T1 and the CDK9 kinase, which, together with other elongation factors, form a "super elongation complex" at the elongating RNA polymerase II that potently activates HIV-1 transcription.<sup>5-7</sup> Tat is the target of latency-promoting therapies,<sup>8,9</sup> and its interactions with TAR and P-TEFb are regulated by a wide variety of post-translational modifications, including phosphorylation, acetylation, methylation, and polyubiquitylation.<sup>10-15</sup>

Latent HIV-1 proviruses are primarily found integrated into actively transcribed genes and yet display heterochromatic features.<sup>16,17</sup> These features include methylation marks in histones associated with the viral promoter located in the 5' long terminal repeat (LTR). KMTs covalently transfer methyl groups from the cofactor S-adenosine methionine (SAM) to lysines within histone or non-histone proteins.<sup>18</sup> However, lysines can be reversibly mono-, di-, or tri-methylated, which results in transcriptional activation or repression, depending on the amino acid residue that is methylated and the state of methylation. More than 50 human KMTs are known or predicted to methylate histones or non-histone substrates; seven of them are known to silence and two to activate HIV-1 transcription by modifying histones or Tat.<sup>19</sup> KMTs, however, represent underexplored therapeutic targets in HIV-1 latency.

Here, we identify a methyltransferase, Su(var)3-9, enhancer-of-zeste, and trithorax (SET) and myeloid, nervy, and DEAF-1 (MYND) domain-containing protein 5 (SMYD5), that activates HIV-1 transcription. Previously, we performed an unbiased small hairpin RNA (shRNA) screen to identify host methyltransferases that contribute to HIV-1 latency in infected T cell lines.<sup>20</sup> We found that knockdown of SMYD5 reproducibly and robustly repressed HIV-1 transcription identifying SMYD5 as a potential transcriptional activator. SMYD5 contains a SET domain that is split by a zinc finger containing the myeloid translocation protein-8, Nervy, and DEAF-1 (MYND) motif followed by a cysteine-rich post-SET domain.<sup>21</sup> Unlike other SMYD family members (SMYD1-SMYD4), SMYD5 lacks a C-terminal tetratricopeptide repeat domain but has a C-terminal glutamate-rich extension instead.<sup>22</sup>

To date, only few papers have been published about SMYD5's role in transcription. For example, SMYD5 associates with NCoR corepressor complexes and tri-methylates histone 4 lysine 20 (H4K20me3) at the promoters of Toll-like receptor 4 (TLR4) target genes in macrophages, thereby negatively regulating inflammatory responses.<sup>23</sup> In addition, histone 3 lysine 36 (H3K36) has been reported as substrate of SMYD5 in two recent publications. A study in mouse embryonic stem cells (mESCs) showed that SMYD5 is recruited to chromatin by RNA polymerase II and catalyzes tri-methylation of H3K36<sup>24</sup>; Aljazi et al.<sup>25</sup> reported that SMYD5 mono-methylates H3K36 and H3K37 (H3K36/K37me1) *in vitro*. The full physiological function of SMYD5 remains largely unknown. In this work, we find that SMYD5 is upregulated in activated CD4<sup>+</sup> T cells and powerfully activates the HIV-1 promoter with and without Tat. While SMYD5 methylates Tat *in vitro* more efficiently than any histone target tested, Tat, through its associated cofactor USP11, increases SMYD5

protein levels in T cells to amplify HIV-1 transcription. We propose that SMYD5 is a critical HIV-1 host activator in activated CD4<sup>+</sup> T cells and a possible target for silencing-promoting therapies.

## RESULTS

### SMYD5 activates HIV-1 transcription in cell lines and primary T cells

To identify epigenetic regulators of HIV-1 latency, we completed a shRNA screen of 46 KMTs and identified 12 whose knockdown suppressed basal or CD3/CD28-induced transcription of the latent HIV-1 LTR.<sup>20</sup> We also participated in a genome-wide screen for cellular latency regulators using a pooled ultracomplex shRNA library with the Verdin and Weissman labs at the Buck Institute, Gladstone Institutes, and University of California San Francisco (UCSF).<sup>26</sup> In both screens, a little-known KMT, SMYD5, was identified as a top activating factor necessary for basal and CD3/CD28-induced HIV-1 transcription. To confirm results from the shRNA screens, we knocked down SMYD5 in the CD4<sup>+</sup> J-Lat 5A8 cell line. This cell line harbors a latent full-length HIV-1 provirus with the fluorescent marker GFP inserted into the *nef* open reading frame, which allows us to monitor the provirus's transcriptional activity by flow cytometry (Figure 1A).<sup>27</sup> HIV-1 transcription can be induced in this cell line with  $\alpha$ CD3/CD28 antibodies, which mimics physiological T cell receptor engagement. The line also closely clustered with patient-derived cells in a study comparing different latency-reversing agents (LRAs) in distinct models of HIV-1 latency.<sup>28</sup>

Cells were transduced with lentiviral vectors expressing two different shRNAs targeting SMYD5 or a non-targeting control, followed by puromycin treatment to select successfully transduced cells. shRNA knockdown was confirmed using western blotting and was ~80% effective (Figure 1B). Cells were then stimulated with medium or saturating doses of  $\alpha$ CD3/CD28 antibodies or left untreated for 24 h, followed by flow cytometry of GFP. Knockdown of SMYD5 effectively suppressed residual HIV-1 expression under basal conditions as well as impaired reactivation of viral transcription at low  $\alpha$ CD3/CD28 concentrations by almost 50% and by up to 75% at high  $\alpha$ CD3/28 concentrations (Figure 1C). Cell viability was monitored by live/death stain and forward/side scatter analysis and showed very little difference between control and SMYD5 knockdown cells (Figure 1D). To control for the specificity of the effect, we performed a SMYD5 rescue experiment. J-Lat 5A8 cells were transduced with SMYD5 shRNAs, selected with puromycin for 3 days, and infected a second time with vesicular stomatitis virus G protein (VSV-G) pseudotyped lentiviruses containing a SMYD5 expression plasmid. After 72 h and 96 h, GFP<sup>+</sup> cells were analyzed by flow cytometry, which showed that SMYD5 overexpression fully restored basal HIV-1 expression in SMYD5 knockdown cells (Figure 1E).

To exclude a cell-dependent effect, we knocked down SMYD5 in two other J-Lat clones, A72 and A2. These clones contain HIV-1 minigenomes composed of just the HIV-1 promoter in the 5' LTR that drives GFP expression (LTR-GFP; A72) or an LTR-Tat-internal ribosome entry site (IRES)-GFP cassette where transcriptional activity is driven by Tat (A2).<sup>29,30</sup> In both cell lines, we observed suppression of GFP expression in cells lacking SMYD5 (Figures S1A–S1D).

We also examined the role of SMYD5 in primary T cells. SMYD5 has been shown to be highly expressed in human CD4<sup>+</sup> T cells.<sup>31</sup> We confirmed this finding in CD4<sup>+</sup> T cells isolated from six independent blood donors (Figures 2A and S2A). Furthermore, we observed that SMYD5 protein expression consistently increases in primary CD4<sup>+</sup> T cells upon activation with  $\alpha$ CD3/CD28 Dynabeads and less consistently with tumor necrosis factor alpha (TNF- $\alpha$ ) treatment (Figures 2A and S2A).

To examine the effect of SMYD5 knockdown in primary CD4<sup>+</sup> T cells, we used modified lentiviral vectors expressing shRNAs against SMYD5 or non-targeting control shRNAs. These vectors express the mCherry protein instead of the puromycin selection marker, which allows identification of successfully transduced cells by flow cytometry.<sup>32,33</sup> Primary CD4<sup>+</sup> T cells isolated from three uninfected blood donors (Figure S2B) were activated with  $\alpha$ CD3/CD28 Dynabeads for 3 days and transduced first with lentiviral particles encoding shRNAs against SMYD5 or non-targeting control shRNAs (Figure 2B). SMYD5 expression was efficiently suppressed in all three donors 3 days after infection (Figure 2E). Transduced CD4<sup>+</sup> T cell cultures were subsequently infected with a molecular clone of the viral isolate HIV-1<sub>NL4-3</sub> (Figure 2B). This virus contains the GFP open reading frame in place of *nef*, allowing identification of infected cells by flow cytometry (Figure S2C), and a frameshift mutation in the *env* gene, thereby restricting infection to a single cycle.<sup>30</sup> Knockdown of SMYD5, as marked by mCherry expression, in all donors caused a reduction in GFP expression compared with cells expressing the non-targeting shRNA control (Figure 2C), confirming that SMYD5 activates HIV-1 transcription in primary T cells. Cell viability was not affected by SMYD5 knockdown (Figure 2D), and SMYD5 knockdown efficiency was confirmed by qRT-PCR (Figure 2E).

### SMYD5 associates with the activated HIV-1 promoter

HIV-1 transcription depends heavily on the viral protein Tat. To test whether SMYD5's effect on HIV-1 was Tat dependent, we overexpressed SMYD5, with or without Tat, in HeLa cells along with a viral LTR-luciferase reporter. We observed a 300-fold increase of LTR activity when SMYD5 was co-expressed with low doses of Tat (Figure 3B). Notably, we observed a 100-fold increase in LTR activity with SMYD5 alone in the absence of Tat (Figure 3A). To demonstrate that this effect is specific for the HIV-1 LTR, we used an EF1 $\alpha$ -*Renilla* luciferase construct and showed that it is insensitive to overexpression of SMYD5 (Figure S3C). These observations led us to hypothesize that SMYD5 associates with the HIV-1 promoter. To test this hypothesis, we carried out chromatin immunoprecipitation (ChIP) experiments in J-Lat cells.

Chromatin was prepared from J-Lat 5A8 cells either unstimulated or stimulated with TNF- $\alpha$ , incubated with SMYD5 or immunoglobulin (IgG) control antibodies, and immunoprecipitated as described previously.<sup>34</sup> DNA extracted from the immunoprecipitated material or the input control was subjected to quantitative PCR analysis with primers specific for the HIV-1 promoter or for the control RPL30 gene.<sup>35</sup> While SMYD5 was not detected associated with the latent HIV-1 promoter, significant enrichment over the input and the IgG control was observed after TNF- $\alpha$  activation, similar to the enrichment of RNA polymerase II (RNA Pol II) after activation (Figure 3C). SMYD5 was not recruited

to the RPL30 gene with or without TNF- $\alpha$ , while *in vivo* association of RNA Pol II was detected after TNF- $\alpha$  treatment (Figure 3D), demonstrating a specific association of SMYD5 with the actively transcribing HIV-1 promoter. The same was observed in the A72 cell line lacking Tat (Figures S3A and S3B). Importantly, RNA Pol II association and recruitment of the CDK9 subunit of P-TEFb were found to be critically dependent on the presence of SMYD5 because binding of both factors was markedly diminished across the HIV-1 LTR after SMYD5 knockdown (Figures 3E, 3F, and S3F). Furthermore, H3K4me3, a histone modification that is associated with transcriptionally active promoters was strongly diminished across the HIV-1 LTR after SMYD5 knockdown, while for H3K36me3, no significant reduction was observed. Collectively, our data identify SMYD5 as an activator of HIV-1 transcription that acts with or without Tat and is physically recruited to the HIV-1 promoter *in vivo* and supports association of RNA Pol II and recruitment of P-TEFb to the HIV-1 promoter, consistent with a possible role in transcription elongation.

### SMYD5 forms a complex with TAR RNA and methylates Tat

The TAR RNA element is a characteristic stem-loop structure at the 5' end of all viral transcripts and recruits the Tat protein to the HIV-1 promoter. To examine whether SMYD5 could also bind TAR, we performed electrophoretic mobility shift assays (EMSAs) with recombinant SMYD5 and radiolabeled TAR RNA as a probe. Surprisingly, addition of SMYD5 alone efficiently shifted the TAR RNA probe, pointing to an RNA-binding property of SMYD5 (Figure 4C). Like Tat, SMYD5 required the bulge region of the TAR stem to bind to TAR RNA (Figure 4C) and was successfully competed off with unlabeled TAR RNA (Figure 4D). This could explain how SMYD5 is recruited to the HIV-1 promoter during HIV-1 transcription.

To identify the protein targets of the SMYD5 methyltransferase activity at the HIV-1 promoter, we performed *in vitro* methylation assays with recombinant SMYD5 and several factors playing a critical role in HIV transcription, such as histones, nuclear factor  $\kappa$ B (NF- $\kappa$ B) RelA, Sp1, and the P-TEFb complex composed of Cyclin T1 and CDK9. We also assessed the *in vitro* methylation of Tat peptides spanning amino acids (aa) 1–72. Reactions included  $^3\text{H}$ -SAM and were performed with or without recombinant SMYD5 enzyme. Following gel electrophoresis, Coomassie staining, and autoradiography, Tat was prominently methylated by SMYD5, while no methylation was detected on NF- $\kappa$ B RelA, Sp1, Cyclin T1, and CDK9 (Figure 4B). In addition, SMYD5 methylated histones H1, H2B, H3, and weakly H4, but not histone H2A, *in vitro* (Figure 4A). Collectively, these data show that SMYD5 can methylate histones and Tat at the HIV-1 promoter and can by itself bind TAR RNA as a possible way of recruitment.

### SMYD5 levels increase in complex with Tat and the Tat cofactor USP11

To investigate how SMYD5 synergizes with Tat, we performed co-immunoprecipitation experiments and found that SMYD5 associated with Tat in cells (Figure 5A and 5B). Interestingly, co-expression of Tat led to an upregulation of SMYD5 protein levels in HEK293T cells overexpressing both proteins (Figure 5C). Similarly, we found that endogenous SMYD5 protein levels were increased in a dose-dependent manner when Tat expression was induced by increasing amounts of TNF- $\alpha$  (Figure 5D). This occurred at

the posttranscriptional level because SMYD5 mRNA levels measured by qRT-PCR were unaffected (Figure 5E).

Ubiquitination, the attachment of ubiquitin to target proteins, is an important regulator of protein stability and cell signaling and is reversed by deubiquitinating enzymes or ubiquitin-specific proteases (USPs). In a large HIV-1: host protein interactome in HEK293T cells, the Tat protein associated with USP11<sup>36</sup> (Figure 6A). This interaction was recently confirmed in a large CRISPR-Cas9-mediated knockout screen in primary human CD4<sup>+</sup> T cells, where USP11 was found to be a potential HIV-1 dependency or restriction factor.<sup>37</sup> USP11 is known to deubiquitinate multiple proteins, including the human papilloma virus (HPV16) E7 protein, where it regulates the levels of E7 protein and subsequently affects the biological function of E7.<sup>38,39</sup> Further, USP11 is implicated in the initiation and progression of several malignancies, including cervical, brain, lung, liver, and colon cancer.<sup>38,40–44</sup> We hypothesized that the stabilization of SMYD5 by Tat may implicate USP11. We confirmed the interaction of USP11 and Tat by co-immunoprecipitating endogenous USP11 with overexpressed Tat in HEK293T cells (Figure 6B). This was not observed with the empty vector control or FLAG-GFP overexpression. Endogenous USP11 also co-immunoprecipitated with overexpressed SMYD5; this was observed regardless of whether Tat was co-expressed and also co-immunoprecipitated with SMYD5 (Figure 6C).

Notably, USP11 was well expressed in primary CD4<sup>+</sup> T cells isolated from the two independent blood donors shown in Figure 2A by western blot analysis and qRT-PCR. The protein and mRNA levels were increased upon activation with  $\alpha$ CD3/CD28 antibodies, while the levels of another deubiquitinase, USP8, remained unchanged (Figure S4A). To examine the functional relevance of USP11 in Tat-mediated SMYD5 upregulation, we performed knockdown experiments with USP11 in HEK293 cells (Figures 6D and 6E). Loss of USP11 resulted in an ~10-fold decrease in SMYD5 upregulation without affecting Tat levels, indicating that USP11 plays a role in causing the increased SMYD5 expression by Tat.

## DISCUSSION

Here, we report that SMYD5, a little-studied methyltransferase with previously reported corepressor function, potently activates the HIV-1 promoter. Our data show inhibition of HIV-1 transcription after shRNA-mediated knockdown of SMYD5 in latently infected T cell lines and primary CD4<sup>+</sup> T cells and *in vivo* association of SMYD5 with the HIV-1 LTR during active transcription. While SMYD5 can bind and activate the HIV-1 LTR by itself and is required for efficient RNA Pol II association and CDK9 recruitment, this effect is amplified in the presence of the viral protein Tat. SMYD5 is not detected to associate with the HIV-1 LTR in non-induced cells, which supports the model where SMYD5 is only lowly expressed but upregulated in expression after induction. We speculate that the documented RNA-binding capacity of SMYD5 could tether low levels of the protein to the HIV-1 LTR in the absence of Tat, which is greatly enhanced after TNF- $\alpha$  stimulation and Tat expression, because more protein is expressed and better recruited to the promoter. Our findings suggest that Tat stabilizes SMYD5 protein levels through deubiquitination by USP11 (Figure 7). SMYD5, in turn, methylates Tat, thereby possibly contributing to



activation of HIV-1 transcription (Figure 7). Because SMYD5 mostly binds to the activated promoter, we propose that SMYD5 is a host factor critically amplifying HIV-1 latency reversal in activated T cells and, therefore, a target for silencing-promoting therapies.

The finding that SMYD5 is a coactivator of HIV-1 transcription was unexpected because Kidder et al. demonstrated SMYD5's corepressor role in mESCs; they found SMYD5 enriched at long interspersed nuclear elements (LINE) and LTR regions and reduced heterochromatin protein  $\alpha$  (HP-1 $\alpha$ ) levels as well as the histone marks H4K20me3 and H3K9me3 in shSmyd5 cells.<sup>45</sup> HP-1 $\alpha$  and H4K20me3 have been implicated in gene silencing.<sup>46,47</sup> Further, the H3K9me3 mark has been linked to HIV-1 latency and has strong ties to heterochromatin formation.<sup>48</sup> However, in some cases, H3K9me3 is permissive to, or even required for, transcription.<sup>49</sup> Other recent findings suggest that H4K20me3 co-localizes with H3K4me3 at a subset of regions, suggesting that H4K20me3 marks transcriptionally dynamic regions in ESCs.<sup>50</sup>

We work in human CD4<sup>+</sup> T cells and show strong cellular expression and *in vivo* recruitment of SMYD5 to the HIV-1 LTR upon activation. Further, we show that SMYD5 *in vitro* methylates all histones, except histone 2A, and only weakly methylates histone 4. We therefore speculate that histone 4 is not the primary target of SMYD5 and that SMYD5 has different action modes depending on the substrate and interaction partner; in our case, the HIV-1 Tat protein. This may also explain why we do not find a difference in H3K36me3 marks in SMYD5 knockdown cells. Such a mechanism of action has been shown previously for another methyltransferase, EZH2. EZH2 catalyzes H3K27me3 dependent on polycomb repressive complex 2 (PCR2), which contributes to transcriptional silencing.<sup>51,52</sup> However, EZH2 is also capable of methylating several non-histone proteins, including STAT3 and talin, which contributes to transcriptional activation.<sup>53,54</sup> The finding that SMYD5 synergizes with Tat to activate the HIV-1 promoter indicates a positive effect of SMYD-mediated methylation on Tat function. Future experiments will map the SMYD5-methylated lysine(s) in Tat and determine their function in Tat-mediated transactivation of the HIV-1 LTR.

USP11 is a so far unrecognized deubiquitinase linked to SMYD5. USP11 has been shown to preferentially cleave K6- and K63-linked ubiquitin chains *in vitro*.<sup>39</sup> K63-linked ubiquitination has non-degradative functions in several processes, including intracellular trafficking, kinase signaling, and DNA damage response, but recently has also been reported to play an important role in lysosomal sorting of several proteins for degradation.<sup>55-57</sup> As we continue the study of USP11 and SMYD5, we will also focus on defining possible ubiquitination modifications of SMYD5. Notably, SMYD5 has been shown to interact with ubiquitin C (UBC),<sup>58,59</sup> and we found that SMYD5 co-immunoprecipitates with ubiquitin (Figure S4B). Future experiments will examine whether SMYD5 is ubiquitinated in cells and whether it is a direct target for the deubiquitinase activity of USP11 and explore the therapeutic potential of SMYD5 or USP11 enzymatic inhibitors in durably silencing HIV-1 transcription.

## Limitations of the study

This study explores the role of SMYD5 in HIV-1 transcription. Although we characterize the cellular interaction between SMYD5 with the viral protein Tat and the host protein USP11 and their effect on HIV-1 transcription, additional work is necessary to translate this into clinical application. One of the limitations of the study is that we performed experiments in shRNA-containing cells with partial knockdown only. We were unable to perform any experiments using a SMYD5 inhibitor. This is due to unavailability of a SMYD5 inhibitor when these experiments were initially planned and performed. We are actively screening for an inhibitor. Therefore, future studies using a SMYD5 inhibitor should examine whether endogenous SMYD5 is an ideal cellular target for durably silencing HIV-1 transcription. Another limitation of the study is that the potential mechanism of action is not fully elucidated. Specifically, determining whether SMYD5 is altering a particular histone mark or modifies another cellular protein, ideally in infected cells, would give better insight into the functional consequences of SMYD5 protein function.

## STAR★METHODS

### RESOURCE AVAILABILITY

**Lead contact**—Further information and requests for resources and reagents should be directed to and will be fulfilled by the lead contact, Melanie Ott (mott@gladstone.ucsf.edu).

**Materials availability**—All unique/stable reagents generated in this study are available from the lead contact with a completed Materials Transfer Agreement.

### Data and code availability

- Data reported in this paper will be shared by the lead contact upon request.
- This paper does not report original code.
- Any additional information required to reanalyze the data reported in this paper is available from the lead contact upon request.

### EXPERIMENTAL MODEL AND SUBJECT DETAILS

**Cell lines**—HEK293T and HeLa cells were obtained from the American Type Culture Collection. J-Lat (clones A2, A72, 5A8) cell lines were provided by the Verdin and Greene laboratories.<sup>27,30</sup> HEK293T and HeLa cells were cultured in DMEM supplemented with 10% FBS (Sigma-Aldrich), 1% L-glutamine (Corning) and 1% penicillin-streptomycin (Corning). J-Lat cells were cultured in RPMI supplemented with 10% FBS, 1% L-glutamine and 1% penicillin-streptomycin. TNF $\alpha$  (Sigma-Aldrich) was used at 0.5–20 ng/ml. Human  $\alpha$ CD3/CD28 Dynabeads (Invitrogen) were used at a ratio of 1 bead per 2 cells.

**Primary CD4<sup>+</sup> T cell cultures**—Human primary CD4<sup>+</sup> T cells were isolated from leukocyte reduction chambers (Vitalant Blood Donation, San Francisco, CA) by negative selection using RosetteSep Human CD4<sup>+</sup> T Cell Enrichment Cocktail (StemCell Technologies). Red blood cells (RBC) were removed by addition of RBC lysis solution (83 mg NH<sub>4</sub>Cl, 10 mg KHCO<sub>3</sub>, 18  $\mu$ l EDTA 5%, ddH<sub>2</sub>O to a final volume of 10 ml) followed

by centrifugation at  $1200 \times g$  for 10 min. Isolated primary CD4<sup>+</sup> T cells were cultured at  $1 \times 10^6$  cells/ml in RPMI 1640 containing 10% FBS, 1% L-glutamine (Corning) and 1% penicillin-streptomycin (Corning) and supplemented with IL-2 (20 U/ml, Sigma-Aldrich).

#### Age and gender of the human donors used for CD4<sup>+</sup> T cell isolation

Age	Gender
68	Male
25	Male
29	Female
27	Male
35	Male
53	Male
65	Female
62	Male
21	Female
78	Male
56	Female
61	Male
76	Male
45	Female
71	Female
74	Male

#### METHOD DETAILS

**Plasmids**—V5-SMYD5-expressing vectors (HsCD00329698, HsCD00829682) were purchased from the DNASU Plasmid repository. The cDNA for WT SMYD5 was amplified and tagged with Flag, HA, or V5 by PCR and ligated into EF-1 $\alpha$ -pBOS vector. The plasmid pLKO.1-mCherry was a gift from Dr. Oskar Laur (Addgene plasmid #128073). Phosphorylated Primers for SMYD5 shRNAs #1 and #2 were annealed and ligated into a pLKO.1-mCherry vector using the AgeI and EcoRI restriction sites. Ligated constructs were transformed into Stbl-3 competent cells (NEB) and correct inserts were confirmed by sequencing.

**ShRNA-mediated knockdown**—ShRNA-expressing lentiviral vectors were purchased from Sigma-Aldrich. The plasmids TRCN0000155095 and TRCN0000156306 were used to deplete SMYD5, and TRCN000007358 and TRCN0000315152 to deplete USP11. The pLKO.1 vector containing a non-targeting shRNA was used as control. Pseudotyped viral stocks were produced in  $2 \times 10^6$  HEK293T cells by co-transfecting 10  $\mu$ g of shRNA-expressing lentiviral vectors, 6.5  $\mu$ g of the lentiviral packaging construct pCMVdelta R8.91 and 3.5  $\mu$ g of VSV-G glycoprotein-expressing vector<sup>65</sup> using X-tremeGENE™ 9 DNA transfection reagent (Sigma-Aldrich), and titered for p24 content. HeLa cells were incubated with virus (1 ng of p24 per  $10^6$  cells) containing shRNAs against SMYD5, USP11 or

non-targeting control for 24 hrs. J-Lat A2, A72, 6.3, 11.1 or 5A8 cells were spininfected at 32°C, 1341g, for 2 hrs with virus (1 ng of p24 per 10<sup>6</sup> cells) containing shRNAs against SMYD5 or scramble control. Infected HeLa or J-Lat cells were selected with puromycin (2 µg/ml, Sigma-Aldrich) for 3–5 days. Knockdown efficiency was determined by western blot and qPCR.

**Viral infections in CD4<sup>+</sup> T cells**—Before infection, CD4<sup>+</sup> T cells (at a concentration of 5 × 10<sup>6</sup>/ml) were activated with Human T-Activator αCD3/CD28 Dynabeads (1 bead per 2 cells) in a CO<sub>2</sub> incubator at 37°C. Three days post-activation, CD4<sup>+</sup> T cells were transduced with lentiviral vectors containing shRNAs against SMYD5 (shSMYD5–1, shSMYD5–2) or the non-targeting shRNA control. These lentiviral vectors also express the mCherry protein. Pseudotyped viral stocks were produced in 40 × 10<sup>6</sup> HEK293T cells by co-transfecting 20 µg of shRNA-expressing lentiviral vectors, 6.5 µg of the lentiviral packaging construct pCMVdelta R8.91 and 3.5 µg of VSV-G glycoprotein-expressing vector<sup>65</sup> using X-tremeGENE™ 9 DNA transfection reagent (Sigma-Aldrich), and titered for p24 content. Typically, 10,000 ng p24<sup>Gag</sup>/ml was used. Spinoculations were performed in 96-well V-bottom plates in volumes of 30 µl. Cells and virus were centrifuged at 800 × g for 2 h at 32 °C. After spinoculation, cells were pooled and cultured at 5 × 10<sup>6</sup> cells/ml in RPMI 1640 containing 10% FBS, 1% L-glutamine (Corning) and 1% penicillin-streptomycin (Corning) and supplemented with IL-2 (20 U/ml). Four days after infection, cells were re-infected with viral particles produced from the molecular clone HIV-1<sub>NL4-3</sub>-GFP. The percentage of GFP+ mCherry+ cells was monitored by flow cytometry three and four days after the second infection.

**Protein extraction and western blot**—Cells were lysed in cold FLAG-IP buffer (50mM Tris-HCl pH 7.4, 150mM NaCl, 1mM EDTA, 1% Triton X-100) supplemented with protease and phosphatase inhibitors and centrifuged at 15,000 × g for 10 min at 4 °C. Supernatant was collected as whole cell extract (WCE). Equal amounts of protein were resolved by SDS-polyacrylamide gel electrophoresis, transferred onto nitrocellulose membranes, and incubated for 4 h in 5% milk blocking buffer. The membranes were incubated with SMYD5, USP11, α-Tubulin, GAPDH, Flag, V5 or Tat antibodies overnight, followed by incubation with a secondary α-rabbit or α-mouse antibody conjugated to HRP at a dilution of 1:10000 for 1 h. Blotted membranes were developed by using Lumi-Light Western Blotting Substrate (Roche) or SuperSignal™ West Femto (Thermo Fisher Scientific) and imaged with *Amersham* Hyperfilm ECL or ChemiDoc Imaging Systems (Bio-Rad). All western blots were performed at least three times.

**Immunoprecipitation**—Cells were lysed in 1ml cold FLAG-IP buffer (50mM Tris-HCl pH 7.4, 150mM NaCl, 1mM EDTA, 1% Triton X-100) supplemented with protease and phosphatase inhibitors and centrifuged at 15,000 × g for 10 min at 4 °C. Cellular debris was pelleted, and the supernatant was recovered. 10% of supernatant was kept as input control, the remaining 90% of lysate was incubated overnight at 4°C with 5 µg V5 antibody of M2-Flag agarose (which was washed 4x with Flag-IP buffer before adding to the lysate). Protein A/G Dynabeads™ were blocked with BSA, washed and resuspended in FLAG-IP buffer. Blocked protein A/G Dynabeads™ beads were added to the V5 immunoprecipitation

and rotated at 4°C for 2 h to collect the V5 antibody. A/G Dynabeads™ agarose beads were washed five times with 1ml Flag-IP buffer, resuspended in 120µl Flag-IP buffer and 40µl 4x Laemmli sample buffer (Bio-Rad). M2-Flag agarose was washed five times with 1ml FLAG-IP buffer, resuspended in 120µl Flag-IP buffer and 40µl 4x Laemmli sample buffer. Immunoprecipitates and input controls were resolved by SDS-polyacrylamide gel electrophoresis and subjected to western blotting.

**RNA isolation, reverse transcription, and quantitative RT-PCR**—RNA was isolated using RNeasy Plus Mini Kit (Qiagen) or Direct-zol RNA Miniprep Kit (Zymo Research) and reverse-transcribed using AMV Reverse Transcriptase (Promega) as per the manufacturer's instructions. Quantitative RT-PCR was carried out using Maxima SYBR Green qPCR Master Mix (Thermo Scientific) on SDS 2.4 software (Applied Biosystems) in a total volume of 12 µL. Primer efficiencies were around 100%. Dissociation curve analysis was performed after the end of the qPCR to confirm the presence of a single and specific product.

**Flow cytometry**—For primary CD4<sup>+</sup> T cells, the percentage of cells that were both GFP<sup>+</sup> and mCherry<sup>+</sup> was monitored by flow cytometry three and four days after the second infection using a BD LSRFortessa™ X-20 Flow Cytometer (BD Biosciences). J-Lat cells were treated with the indicated concentration of drugs or left untreated. After 18 h, the percentage of GFP<sup>+</sup> cells was determined using a MACSQuant VYB FACS analyzer (Miltenyi Biotech GmbH) or FACSCalibur Flow Cytometer (BD Biosciences). Cell viability of primary CD4<sup>+</sup> T cells and J-Lat cells was monitored by eBioscience™ fixable viability dye eFluor™ 780 (Invitrogen) and forward-and-side scatter measurement. Analysis was conducted on 3 × 20,000–1Mio. live cells per condition. Data were analyzed using FlowJo 9.5 to 10.8 (Tree Star). All flow cytometry sorting gate strategies are provided in Figure S2.

**In-vitro methylation assays**—For methylation assays, 2 µg of histones (purchased from NEB), recombinant proteins p65, SP1 (both Active Motif), Cyclin T1/CDK9 (Sigma-Aldrich) or synthetic Tat peptides (M. Schnolzer, German Cancer Research Center Heidelberg, Germany) were incubated with recombinant SMYD5 (Active Motif) in a buffer containing 50 mM Tris-HCl, pH 9, 0.01% Tween 20, 2 mM DTT and 1.1 µCi of H<sup>3</sup>-labeled SAM (Perkin Elmer) for 2hr at 30°C. Reaction mixtures were fractionated on 15% SDS-PAGE for proteins or on 10–20% Tris-Tricine gradient gels for peptides (BioRad). After Coomassie staining, gels were treated with Amplify (GE Healthcare) for 30 min, dried and exposed to *Amersham* Hyperfilm (GE Healthcare) overnight.

**RNA electrophoretic mobility shift assays (EMSA)**—TAR RNAs (WT, bulge and loop) were synthesized in *in-vitro* transcription reactions with the Riboprobe system (Promega).<sup>35</sup> Transcripts were treated with 2 U of DNase I (Promega), extracted with a phenol:chloroform mixture and purified over an Illustra MicroSpin G50 column (GE Healthcare). Gel-mobility reactions (12 µl final volume) were carried out in binding buffer (50 mM Tris, pH 7.4, 0.5 mM EGTA, 150 mM NaCl, 2% glycerol, 0.2% Tween 20, 0.5 mM DTT, 90 mM ZnSO<sub>4</sub>, 0.005% BSA and 100 µM ATP) and contained 2×10<sup>4</sup> cpm TAR probes/reaction and the indicated concentrations of Tat and recombinant SMYD5 (Active

Motif). Reactions were incubated for 30 min at 30 °C and separated on a pre-run 4% Tris-glycine gel. The gels were dried and exposed to *Amersham* Hyperfilm (GE Healthcare) overnight.

**Chromatin immunoprecipitation**—J-Lat 5A8, A2 and A72 cells were treated with TNF $\alpha$  (10 ng/ml) for 18 h. Cells were fixed with 1% formaldehyde (v/v) in fixation buffer (1 mM EDTA, 0.5 mM EGTA, 50 mM Hepes, pH 8.0, 100 mM NaCl), and fixation was stopped after 10 min by addition of glycine to 125 mM. The cell membrane was lysed for 15 min on ice (5 mM Pipes, pH 8.0, 85 mM KCl, 0.5% NP40, protease inhibitors). After washing with nuclear swell buffer (25 mM HEPES, pH 7.5, 4 mM KCl, 1 mM DTT, 0.5% NP-40, 0.5 mM PMSF) and micrococcal nuclease (MNase) digestion buffer (20 mM Tris pH 7.5, 2.5 mM CaCl<sub>2</sub>, 5 mM NaCl, 1 mM DTT, 0.5 % NP-40), the pellet was resuspended in MNase buffer (15 mM Tris-HCl, pH 7.5, 5 mM MgCl<sub>2</sub>, 1 mM CaCl<sub>2</sub>, and 25 mM NaCl). Subsequently, samples were incubated with MNase (New England Biolabs) for 10 min at RT. The reaction was quenched with 0.5 M EDTA and incubated on ice for 5 min. Cells were lysed (1% SDS, 10 mM EDTA, 50 mM Tris-HCl, pH 8.1, protease inhibitors), and chromatin DNA was sheared to 200–1000-bp average size through sonication (Ultrasonic Processor CP-130, Cole Parmer). Cellular debris was pelleted, and the supernatant was recovered. Protein A/G Dynabeads were blocked with single-stranded salmon sperm DNA (10  $\mu$ g/ml) and BSA (10  $\mu$ g/ml), washed and resuspended in immunoprecipitation buffer. Blocked protein A/G Dynabeads were added to the digested chromatin fractions and rotated at 4°C for 2 h to preclear chromatin. Lysates were incubated overnight at 4°C with 5–10  $\mu$ g of SMYD5, NF $\kappa$ B RelA, Pol II antibodies, or IgG control. After incubation with protein A/G Dynabeads for 2 h and washing three times with low salt buffer (0.1% SDS, 1% Triton X-100, 2 mM EDTA, 20 mM Tris-HCl, pH 8.1, 150 mM NaCl), one time with high salt buffer (0.1% SDS, 1% Triton X-100, 2 mM EDTA, 20 mM Tris-HCl, pH 8.1, 500 mM NaCl) and twice with TE-buffer (1 mM EDTA, 10 mM Tris-HCl, pH 8.1). Proteins were eluted from A/G Dynabeads and lysates and input DNA were treated with RNase H (New England Biolabs) and Proteinase K (Sigma-Aldrich) at 37 °C for 30 min. Crosslinks were reversed with 0.2 M NaCl and by incubating 12–16 hours at 65°C in a thermoshaker. Chromatin was recovered with Agencourt AMPure XP beads (Beckman Coulter). Immunoprecipitated chromatin was quantified by real-time PCR using the Maxima SYBR Green qPCR Master Mix (Thermo Scientific) and the ABI 7700 Sequence Detection System (Applied Biosystems). The SDS 2.4 software (Applied Biosystems) was used for analysis. The specificity of each PCR reaction was confirmed by melting curve analysis using the Dissociation Curve software (Applied Biosystems). All chromatin immunoprecipitations and qPCRs were repeated at least three times, and representative results were shown. Primer sequences are listed in the key resources table.

**Luciferase assays**— $3 \times 10^5$  HeLa cells were transfected with 25 ng HIV-LTR-Luc, 0.25–250 ng SMYD5 WT and 2 ng WT Tat-expressing plasmids or corresponding amounts of the empty vector (EF-1 $\alpha$ -pBOS) using X-tremeGENE™ 9 DNA transfection reagent (Sigma-Aldrich, Roche Diagnostics) following manufacturer instructions. Cells were harvested 48 h after infection, washed one time with PBS, and lysed in 110  $\mu$ l of Passive Lysis Buffer (Luciferase Assay System, Promega). After 30 min of lysis, the supernatant was harvested

and the luciferase activity in cell extract was quantified with a SpectraMax i3x plate reader and SoftMax Pro 6.5.1 software after mixing 20  $\mu$ l of lysate with 100  $\mu$ l of substrate (Luciferase Assay System, Dual-Luciferase Assay System, Promega). Relative light units (RLU) were normalized to protein content determined by DC™ Protein assay (Bio-Rad). ANOVA tests were performed to calculate statistical significance.

## QUANTIFICATION AND STATISTICAL ANALYSIS

All values are depicted as mean  $\pm$  SD. Statistical parameters including statistical analysis, statistical significance, and n value are reported in the Figure legends and Supplementary Figure legends. Statistical analyses were performed using Prism Software (GraphPad). The average of three independent experiments analyzed in triplicate  $\pm$  SEM is shown and compared with control samples by ANOVA: \* $p < 0.05$ , \*\* $p < 0.005$ , \*\*\* $p < 0.001$ . For statistical analysis of T-cell activation experiments 1-way ANOVA with Dunnett's multiple comparison test  $p < 0.01$ ,  $n = 4$  was employed.

## Supplementary Material

Refer to Web version on PubMed Central for supplementary material.

## ACKNOWLEDGMENTS

We thank members of the Ott, Marson, Krogan, and Greene laboratories for helpful discussions, reagents, and expertise. We thank J. Srivastava, N. Raman, and the Gladstone Flow Cytometry Core for assistance with flow cytometry; J. Carroll for graphics; F. Chanut for editorial assistance; and V. Fonseca and L. Weiser for administrative assistance. This work was supported by the National Institutes of Health/National Institute of Allergy and Infectious Diseases (NIH/NIAID; DP1DA038043 and R37AI083139 to M.O.), the NIH/National Institute on Drug Abuse (R01DA043142), and the NIH (P30 AI027763 to the Flow Cytometry Core). The work was also supported by the UCSF Aids Research Institute with funding from amfAR (109301–59-RGRL). D.B. was also funded by the Gilead HIV Cure Mentored Scientist Award from the UCSF AIDS Research Institute. Further, we gratefully acknowledge support from the HOPE Collaboratory (UM1AI164559 to M.O.) and the James B. Pendleton Charitable Trust.

## INCLUSION AND DIVERSITY

We support inclusive, diverse, and equitable conduct of research.

## REFERENCES

1. Mbonye U, and Karn J (2014). Transcriptional control of HIV latency: cellular signaling pathways, epigenetics, happenstance and the hope for a cure. *Virology* 454–455, 328–339. 10.1016/j.virol.2014.02.008.
2. Blazkova J, Trejbalova K, Gondois-Rey F, Halfon P, Philibert P, Guiguen A, Verdin E, Olive D, Van Lint C, Hejnar J, and Hirsch I (2009). CpG methylation controls reactivation of HIV from latency. *PLoS Pathog.* 5, e1000554. 10.1371/journal.ppat.1000554. [PubMed: 19696893]
3. Kauder SE, Bosque A, Lindqvist A, Planelles V, and Verdin E (2009). Epigenetic regulation of HIV-1 latency by cytosine methylation. *PLoS Pathog.* 5, e1000495. 10.1371/journal.ppat.1000495. [PubMed: 19557157]
4. Verdin E, Paras P Jr., and Van Lint C (1993). Chromatin disruption in the promoter of human immunodeficiency virus type 1 during transcriptional activation. *EMBO J.* 12, 3249–3259. [PubMed: 8344262]

5. Sobhian B, Laguette N, Yatim A, Nakamura M, Levy Y, Kiernan R, and Benkirane M (2010). HIV-1 Tat assembles a multifunctional transcription elongation complex and stably associates with the 7SK snRNP. *Mol. Cell* 38, 439–451. 10.1016/j.molcel.2010.04.012. [PubMed: 20471949]
6. Marzio G, Tyagi M, Gutierrez MI, and Giacca M (1998). HIV-1 tat transactivator recruits p300 and CREB-binding protein histone acetyltransferases to the viral promoter. *Proc. Natl. Acad. Sci. USA* 95, 13519–13524. [PubMed: 9811832]
7. Lusic M, Marcello A, Cereseto A, and Giacca M (2003). Regulation of HIV-1 gene expression by histone acetylation and factor recruitment at the LTR promoter. *EMBO J.* 22, 6550–6561. 10.1093/emboj/cdg631. [PubMed: 14657027]
8. Mousseau G, Kessing CF, Fromentin R, Trautmann L, Chomont N, and Valente ST (2015). The tat inhibitor didehydro-cortistatin A prevents HIV-1 reactivation from latency. *mBio* 6, e00465. 10.1128/mBio.00465-15. [PubMed: 26152583]
9. Mousseau G, and Valente S (2012). Strategies to block HIV transcription: focus on small molecule tat inhibitors. *Biology* 1, 668–697. 10.3390/biology1030668. [PubMed: 24832514]
10. Endo-Munoz L, Warby T, Harrich D, and McMillan NAJ (2005). Phosphorylation of HIV Tat by PKR increases interaction with TAR RNA and enhances transcription. *Viol. J.* 2, 17. 10.1186/1743-422X-2-17. [PubMed: 15737233]
11. Kiernan RE, Vanhulle C, Schiltz L, Adam E, Xiao H, Maudoux F, Calomme C, Burny A, Nakatani Y, Jeang KT, et al. (1999). HIV-1 tat transcriptional activity is regulated by acetylation. *EMBO J.* 18, 6106–6118. 10.1093/emboj/18.21.6106. [PubMed: 10545121]
12. Ott M, Schnölzer M, Garnica J, Fischle W, Emiliani S, Rackwitz HR, and Verdin E (1999). Acetylation of the HIV-1 Tat protein by p300 is important for its transcriptional activity. *Curr. Biol.* 9, 1489–1492. [PubMed: 10607594]
13. Brès V, Kiernan RE, Linares LK, Chable-Bessia C, Plechakova O, Tréand C, Emiliani S, Peloponese JM, Jeang KT, Coux O, et al. (2003). A non-proteolytic role for ubiquitin in Tat-mediated transactivation of the HIV-1 promoter. *Nat. Cell Biol.* 5, 754–761. 10.1038/ncb1023. [PubMed: 12883554]
14. Xie B, Invernizzi CF, Richard S, and Wainberg MA (2007). Arginine methylation of the human immunodeficiency virus type 1 Tat protein by PRMT6 negatively affects Tat Interactions with both cyclin T1 and the Tat transactivation region. *J. Virol.* 81, 4226–4234. 10.1128/JVI.01888-06. [PubMed: 17267505]
15. Sivakumaran H, van der Horst A, Fulcher AJ, Apolloni A, Lin MH, Jans DA, and Harrich D (2009). Arginine methylation increases the stability of human immunodeficiency virus type 1 Tat. *J. Virol.* 83, 11694–11703. 10.1128/JVI.00499-09. [PubMed: 19726520]
16. Han Y, Lassen K, Monie D, Sedaghat AR, Shimoji S, Liu X, Pierson TC, Margolick JB, Siliciano RF, and Siliciano JD (2004). Resting CD4+ T cells from human immunodeficiency virus type 1 (HIV-1)-infected individuals carry integrated HIV-1 genomes within actively transcribed host genes. *J. Virol.* 78, 6122–6133. 10.1128/JVI.78.12.6122-6133.2004. [PubMed: 15163705]
17. Lewinski MK, Yamashita M, Emerman M, Ciuffi A, Marshall H, Crawford G, Collins F, Shinn P, Leipzig J, Hannenhalli S, et al. (2006). Retroviral DNA integration: viral and cellular determinants of target-site selection. *PLoS Pathog.* 2, e60. 10.1371/journal.ppat.0020060. [PubMed: 16789841]
18. Kouzarides T (2007). Chromatin modifications and their function. *Cell* 128, 693–705. 10.1016/j.cell.2007.02.005. [PubMed: 17320507]
19. Boehm D, and Ott M (2017). Host methyltransferases and demethylases: potential new epigenetic targets for HIV cure strategies and beyond. *AIDS Res. Hum. Retrovir.* 33, S8–S22. 10.1089/aid.2017.0180. [PubMed: 29140109]
20. Boehm D, Jeng M, Camus G, Gramatica A, Schwarzer R, Johnson JR, Hull PA, Montano M, Sakane N, Pagans S, et al. (2017). SMYD2-Mediated histone methylation contributes to HIV-1 latency. *Cell Host Microbe* 21, 569–579.e6. 10.1016/j.chom.2017.04.011. [PubMed: 28494238]
21. Brown MA, Sims RJ 3rd, Gottlieb PD, and Tucker PW (2006). Identification and characterization of Smyd2: a split SET/MYND domain-containing histone H3 lysine 36-specific methyltransferase that interacts with the Sin3 histone deacetylase complex. *Mol. Cancer* 5, 26. 10.1186/1476-4598-5-26. [PubMed: 16805913]



22. Abu-Farha M, Lanouette S, Elisma F, Tremblay V, Butson J, Figeys D, and Couture JF (2011). Proteomic analyses of the SMYD family interactomes identify HSP90 as a novel target for SMYD2. *J. Mol. Cell Biol.* 3, 301–308. 10.1093/jmcb/mjr025.
23. Stender JD, Pascual G, Liu W, Kaikkonen MU, Do K, Spann NJ, Boutros M, Perrimon N, Rosenfeld MG, and Glass CK (2012). Control of proinflammatory gene programs by regulated trimethylation and demethylation of histone H4K20. *Mol. Cell* 48, 28–38. 10.1016/j.molcel.2012.07.020. [PubMed: 22921934]
24. Zhang Y, Fang Y, Tang Y, Han S, Jia J, Wan X, Chen J, Yuan Y, Zhao B, and Fang D (2022). SMYD5 catalyzes histone H3 lysine 36 tri-methylation at promoters. *Nat. Commun.* 13, 3190. 10.1038/s41467-022-30940-1. [PubMed: 35680905]
25. Aljazi MB, Gao Y, Wu Y, and He J (2022). SMYD5 is a histone H3-specific methyltransferase mediating mono-methylation of histone H3 lysine 36 and 37. *Biochem. Biophys. Res. Commun.* 599, 142–147. 10.1016/j.bbrc.2022.02.043. [PubMed: 35182940]
26. Besnard E HS, Kampmann M, Lim HW, Hosmane NN, Martin A, Bassik MC, Verschueren E, Battivelli E, Chan J, Stevensson JP, et al. (2016). Genome-wide shRNA profiling reveals a novel role for mTOR in HIV latency. *Cell Host Microbe* 20, 700–702. [PubMed: 27978431]
27. Chan JK, Bhattacharyya D, Lassen KG, Ruelas D, and Greene WC (2013). Calcium/calcineurin synergizes with prostratin to promote NF-kappaB dependent activation of latent HIV. *PLoS One* 8, e77749. 10.1371/journal.pone.0077749. [PubMed: 24204950]
28. Spina CA, Anderson J, Archin NM, Bosque A, Chan J, Famiglietti M, Greene WC, Kashuba A, Lewin SR, Margolis DM, et al. (2013). An in-depth comparison of latent HIV-1 reactivation in multiple cell model systems and resting CD4+ T cells from aviremic patients. *PLoS Pathog.* 9, e1003834. 10.1371/journal.ppat.1003834. [PubMed: 24385908]
29. Jordan A, Defechereux P, and Verdin E (2001). The site of HIV-1 integration in the human genome determines basal transcriptional activity and response to Tat transactivation. *EMBO J.* 20, 1726–1738. 10.1093/emboj/20.7.1726. [PubMed: 11285236]
30. Jordan A, Bisgrove D, and Verdin E (2003). HIV reproducibly establishes a latent infection after acute infection of T cells in vitro. *EMBO J.* 22, 1868–1877. [PubMed: 12682019]
31. Kim MS, Pinto SM, Getnet D, Nirujogi RS, Manda SS, Chaerkady R, Madugundu AK, Kelkar DS, Isserlin R, Jain S, et al. (2014). A draft map of the human proteome. *Nature* 509, 575–581. 10.1038/nature13302. [PubMed: 24870542]
32. Grskovic M, Chaivorapol C, Gaspar-Maia A, Li H, and Ramalho-Santos M (2007). Systematic identification of cis-regulatory sequences active in mouse and human embryonic stem cells. *PLoS Genet.* 3, e145. [PubMed: 17784790]
33. Ventura A, Meissner A, Dillon CP, McManus M, Sharp PA, Van Parijs L, Jaenisch R, and Jacks T (2004). Cre-lox-regulated conditional RNA interference from transgenes. *Proc. Natl. Acad. Sci. USA* 101, 10380–10385. [PubMed: 15240889]
34. Schröder S, Herker E, Itzen F, He D, Thomas S, Gilchrist DA, Kaehlcke K, Cho S, Pollard KS, Capra JA, et al. (2013). Acetylation of RNA polymerase II regulates growth-factor-induced gene transcription in mammalian cells. *Mol. Cell* 52, 314–324. 10.1016/j.molcel.2013.10.009. [PubMed: 24207025]
35. Kaehlcke K, Dorr A, Hetzer-Egger C, Kiermer V, Henklein P, Schnoelzer M, Lorent E, Cole PA, Verdin E, and Ott M (2003). Acetylation of Tat defines a cyclinT1-independent step in HIV transactivation. *Mol. Cell* 12, 167–176. [PubMed: 12887902]
36. Jäger S, Cimercancic P, Gulbahce N, Johnson JR, McGovern KE, Clarke SC, Shales M, Mercenne G, Pache L, Li K, et al. (2011). Global landscape of HIV-human protein complexes. *Nature* 481, 365–370. 10.1038/nature10719. [PubMed: 22190034]
37. Hiatt J, Hultquist JF, McGregor MJ, Bouhaddou M, Leenay RT, Simons LM, Young JM, Haas P, Roth TL, Tobin V, et al. (2022). A functional map of HIV-host interactions in primary human T cells. *Nat. Commun.* 13, 1752. 10.1038/s41467-022-29346-w. [PubMed: 35365639]
38. Lin CH, Chang HS, and Yu WCY (2008). USP11 stabilizes HPV-16E7 and further modulates the E7 biological activity. *J. Biol. Chem.* 283, 15681–15688. 10.1074/jbc.M708278200. [PubMed: 18408009]

39. Harper S, Gratten HE, Cornaciu I, Oberer M, Scott DJ, Emsley J, and Dreveny I (2014). Structure and catalytic regulatory function of ubiquitin specific protease 11 N-terminal and ubiquitin-like domains. *Biochemistry* 53, 2966–2978. 10.1021/bi500116x. [PubMed: 24724799]
40. Wu HC, Lin YC, Liu CH, Chung HC, Wang YT, Lin YW, Ma HI, Tu PH, Lawler SE, and Chen RH (2014). USP11 regulates PML stability to control Notch-induced malignancy in brain tumours. *Nat. Commun.* 5, 3214. 10.1038/ncomms4214. [PubMed: 24487962]
41. Wang D, Zhao J, Li S, Wei J, Nan L, Mallampalli RK, Weathington NM, Ma H, and Zhao Y (2018). Phosphorylated E2F1 is stabilized by nuclear USP11 to drive Peg10 gene expression and activate lung epithelial cells. *J. Mol. Cell Biol.* 10, 60–73. 10.1093/jmcb/mjx034.
42. Zhou Z, Luo A, Shrivastava I, He M, Huang Y, Bahar I, Liu Z, and Wan Y (2017). Regulation of XIAP turnover reveals a role for USP11 in promotion of tumorigenesis. *EBioMedicine* 15, 48–61. 10.1016/j.ebiom.2016.12.014. [PubMed: 28040451]
43. Jacko AM, Nan L, Li S, Tan J, Zhao J, Kass DJ, and Zhao Y (2016). De-ubiquitinating enzyme, USP11, promotes transforming growth factor beta-1 signaling through stabilization of transforming growth factor beta receptor II. *Cell Death Dis.* 7, e2474. 10.1038/cddis.2016.371. [PubMed: 27853171]
44. Deng T, Yan G, Song X, Xie L, Zhou Y, Li J, Hu X, Li Z, Hu J, Zhang Y, et al. (2018). Deubiquitylation and stabilization of p21 by USP11 is critical for cell-cycle progression and DNA damage responses. *Proc. Natl. Acad. Sci. USA* 115, 4678–4683. 10.1073/pnas.1714938115. [PubMed: 29666278]
45. Kidder BL, He R, Wangsa D, Padilla-Nash HM, Bernardo MM, Sheng S, Ried T, and Zhao K (2017). SMYD5 controls heterochromatin and chromosome integrity during embryonic stem cell differentiation. *Cancer Res.* 77, 6729–6745. 10.1158/0008-5472.CAN-17-0828. [PubMed: 28951459]
46. Aagaard L, Laible G, Selenko P, Schmid M, Dorn R, Schotta G, Kuhfittig S, Wolf A, Lebersorger A, Singh PB, et al. (1999). Functional mammalian homologues of the Drosophila PEV-modifier Su(var)3–9 encode centromere-associated proteins which complex with the heterochromatin component M31. *EMBO J.* 18, 1923–1938. 10.1093/emboj/18.7.1923. [PubMed: 10202156]
47. van Nuland R, and Gozani O (2016). Histone H4 lysine 20 (H4K20) methylation, expanding the signaling potential of the proteome one methyl moiety at a time. *Mol. Cell. Proteomics* 15, 755–764. 10.1074/mcp.R115.054742. [PubMed: 26598646]
48. du Chéné I, Basyuk E, Lin YL, Triboulet R, Knezevich A, Chable-Bessia C, Mettling C, Baillat V, Reynes J, Corbeau P, et al. (2007). Suv39H1 and HP1gamma are responsible for chromatin-mediated HIV-1 transcriptional silencing and post-integration latency. *EMBO J.* 26, 424–435. 10.1038/sj.emboj.7601517. [PubMed: 17245432]
49. Vakoc CR, Mandat SA, Olenchock BA, and Blobel GA (2005). Histone H3 lysine 9 methylation and HP1gamma are associated with transcription elongation through mammalian chromatin. *Mol. Cell* 19, 381–391. 10.1016/j.molcel.2005.06.011. [PubMed: 16061184]
50. Xu J, and Kidder BL (2018). H4K20me3 co-localizes with activating histone modifications at transcriptionally dynamic regions in embryonic stem cells. *BMC Genom.* 19, 514. 10.1186/s12864-018-4886-4.
51. Margueron R, and Reinberg D (2011). The Polycomb complex PRC2 and its mark in life. *Nature* 469, 343–349. 10.1038/nature09784. [PubMed: 21248841]
52. Cao R, and Zhang Y (2004). The functions of E(Z)/EZH2-mediated methylation of lysine 27 in histone H3. *Curr. Opin. Genet. Dev.* 14, 155–164. 10.1016/j.gde.2004.02.001. [PubMed: 15196462]
53. Kim E, Kim M, Woo DH, Shin Y, Shin J, Chang N, Oh YT, Kim H, Rhee J, Nakano I, et al. (2013). Phosphorylation of EZH2 activates STAT3 signaling via STAT3 methylation and promotes tumorigenicity of glioblastoma stem-like cells. *Cancer Cell* 23, 839–852. 10.1016/j.ccr.2013.04.008. [PubMed: 23684459]
54. Gunawan M, Venkatesan N, Loh JT, Wong JF, Berger H, Neo WH, Li LYJ, La Win MK, Yau YH, Guo T, et al. (2015). The methyltransferase Ezh2 controls cell adhesion and migration through direct methylation of the extranuclear regulatory protein talin. *Nat. Immunol.* 16, 505–516. 10.1038/ni.3125. [PubMed: 25751747]

55. Geetha T, Jiang J, and Wooten MW (2005). Lysine 63 polyubiquitination of the nerve growth factor receptor TrkA directs internalization and signaling. *Mol. Cell* 20, 301–312. 10.1016/j.molcel.2005.09.014. [PubMed: 16246731]
56. Duncan LM, Piper S, Dodd RB, Saville MK, Sanderson CM, Luzio JP, and Lehner PJ (2006). Lysine-63-linked ubiquitination is required for endolysosomal degradation of class I molecules. *EMBO J.* 25, 1635–1645. 10.1038/sj.emboj.7601056. [PubMed: 16601694]
57. Varghese B, Barriere H, Carbone CJ, Banerjee A, Swaminathan G, Plotnikov A, Xu P, Peng J, Goffin V, Lukacs GL, and Fuchs SY (2008). Polyubiquitination of prolactin receptor stimulates its internalization, postinternalization sorting, and degradation via the lysosomal pathway. *Mol. Cell Biol.* 28, 5275–5287. 10.1128/MCB.00350-08. [PubMed: 18573876]
58. Danielsen JMR, Sylvestersen KB, Bekker-Jensen S, Szklarczyk D, Poulsen JW, Horn H, Jensen LJ, Mailand N, and Nielsen ML (2011). Mass spectrometric analysis of lysine Ubiquitylation reveals promiscuity at site level. *Mol. Cell. Proteomics* 10, M110.003590. 10.1074/mcp.M110.003590.
59. Kim W, Bennett EJ, Huttlin EL, Guo A, Li J, Possemato A, Sowa ME, Rad R, Rush J, Comb MJ, et al. (2011). Systematic and quantitative assessment of the ubiquitin-modified proteome. *Mol. Cell* 44, 325–340. 10.1016/j.molcel.2011.08.025. [PubMed: 21906983]
60. Kutsch O, Benveniste EN, Shaw GM, and Levy DN (2002). Direct and quantitative single-cell analysis of human immunodeficiency virus type 1 reactivation from latency. *J. Virol.* 76, 8776–8786. [PubMed: 12163598]
61. Pagans S, Pedal A, North BJ, Kaehlcke K, Marshall BL, Dorr A, Hetzer-Egger C, Henklein P, Frye R, McBurney MW, et al. (2005). SIRT1 regulates HIV transcription via Tat deacetylation. *PLoS Biol.* 3, e41. 10.1371/journal.pbio.0030041. [PubMed: 15719057]
62. Rafati H, Parra M, Hakre S, Moshkin Y, Verdin E, and Mahmoudi T (2011). Repressive LTR nucleosome positioning by the BAF complex is required for HIV latency. *PLoS Biol.* 9, e1001206. 10.1371/journal.pbio.1001206. [PubMed: 22140357]
63. Drenan RM, Nashmi R, Imoukhuede P, Just H, McKinney S, and Lester HA (2008). Subcellular trafficking, pentameric assembly, and subunit stoichiometry of neuronal nicotinic acetylcholine receptors containing fluorescently labeled alpha6 and beta3 subunits. *Mol. Pharmacol.* 73, 27–41. 10.1124/mol.107.039180. [PubMed: 17932221]
64. Zhuang J, Jetzt AE, Sun G, Yu H, Klarmann G, Ron Y, Preston BD, and Dougherty JP (2002). Human immunodeficiency virus type 1 recombination: rate, fidelity, and putative hot spots. *J. Virol.* 76, 11273–11282. 10.1128/jvi.76.22.11273-11282.2002. [PubMed: 12388687]
65. Naldini L, Blömer U, Gallay P, Ory D, Mulligan R, Gage FH, Verma IM, and Trono D (1996). In vivo gene delivery and stable transduction of nondividing cells by a lentiviral vector. *Science* 272, 263–267. [PubMed: 8602510]
66. Pagans S, Kauder SE, Kaehlcke K, Sakane N, Schroeder S, Dormeyer W, Trievel RC, Verdin E, Schnolzer M, and Ott M (2010). The Cellular lysine methyltransferase Set7/9-KMT7 binds HIV-1 TAR RNA, monomethylates the viral transactivator Tat, and enhances HIV transcription. *Cell Host Microbe* 7, 234–244. 10.1016/j.chom.2010.02.005. [PubMed: 20227666]
67. Sowa ME, Bennett EJ, Gygi SP, and Harper JW (2009). Defining the human deubiquitinating enzyme interaction landscape. *Cell* 138, 389–403. 10.1016/j.cell.2009.04.042. [PubMed: 19615732]
68. Kasler HG, Lee IS, Lim HW, and Verdin E (2018). Histone Deacetylase 7 mediates tissue-specific autoimmunity via control of innate effector function in invariant Natural Killer T Cells. *Elife* 7, e32109. 10.7554/eLife.32109. [PubMed: 29664401]
69. Van Lint C, Amella CA, Emiliani S, John M, Jie T, and Verdin E (1997). Transcription factor binding sites downstream of the human immunodeficiency virus type 1 transcription start site are important for virus infectivity. *J. Virol.* 71, 6113–6127. 10.1128/JVI.71.8.6113-6127.1997. [PubMed: 9223506]

### Highlights

- Lysine methyltransferase SMYD5 knockdown inhibits HIV-1 reactivation from latency
- SMYD5 associates with the HIV-1 LTR and activates transcription
- RNA Pol II and CDK9 associate in a SMYD5-dependent manner with the HIV-1 LTR
- SMYD5 methylates Tat and is stabilized by Tat through USP11

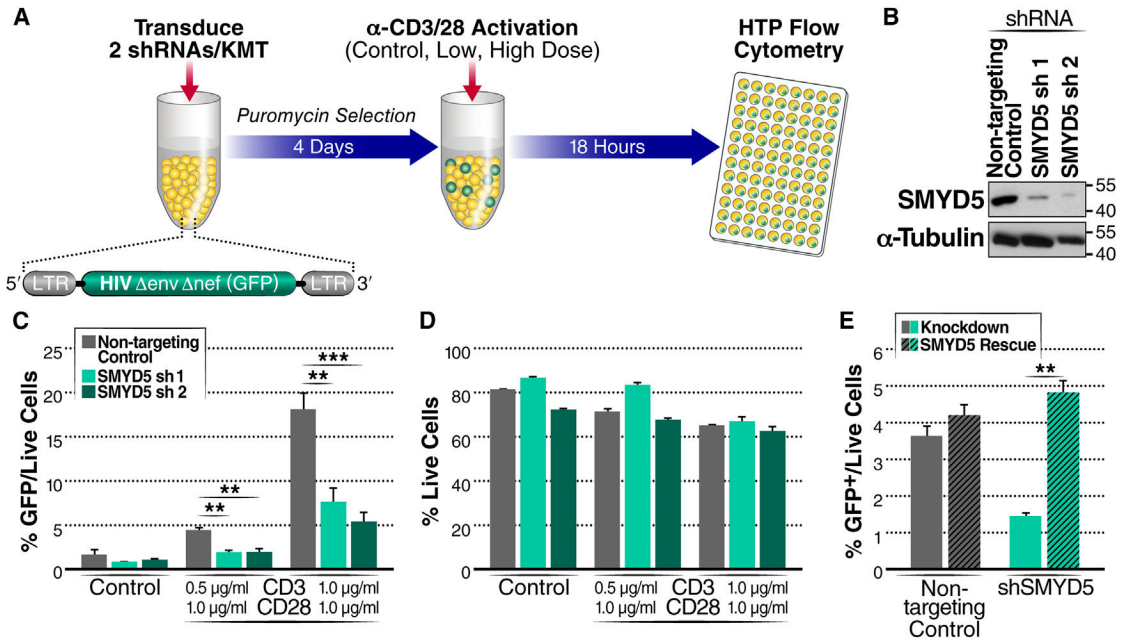


**Figure 1. SMYD5 knockdown inhibits HIV-1 reactivation from latency in J-Lat cells**

(A) Schematic of the workflow. J-Lat 5A8 cells were transduced with SMYD5 shRNA, puromycin selected, and activated with  $\alpha$ CD3/CD28 antibodies for 18 h, and GFP<sup>+</sup> cells were analyzed by flow cytometry.

(B) SMYD5 protein levels in J-Lat 5A8 cells after targeting its RNA with two different lentiviral shRNAs or a non-targeting control.

(C) Reactivation of the latent HIV-1 reporter as measured by GFP flow cytometry. Both SMYD5 shRNAs suppress HIV-1 reactivation under basal conditions and upon activation with  $\alpha$ CD3/CD28. The average of three independent experiments analyzed in triplicate  $\pm$ SEM is shown and compared with control samples by ANOVA: \*\* $p < 0.005$ , \*\*\* $p < 0.001$ .

(D) Cell viability (percentage of live cells), as monitored by forward and side scatter analysis and viability stain, under the same conditions as in (C). The average of three independent experiments analyzed in triplicate  $\pm$  SEM is shown.

(E) J-Lat 5A8 cells were transduced with SMYD5 shRNA, puromycin selected for 3 days, and infected a second time with VSV-G pseudotyped virus containing aSMYD5 expression plasmid. After 72 h and 96 h, GFP<sup>+</sup> cells were analyzed by flow cytometry. SMYD5 overexpression restores HIV-1 reactivation in SMYD5 knockdown cells under basal conditions. The average of three independent experiments analyzed in triplicate  $\pm$ SEM is shown and compared with control samples by ANOVA: \*\* $p < 0.005$ .

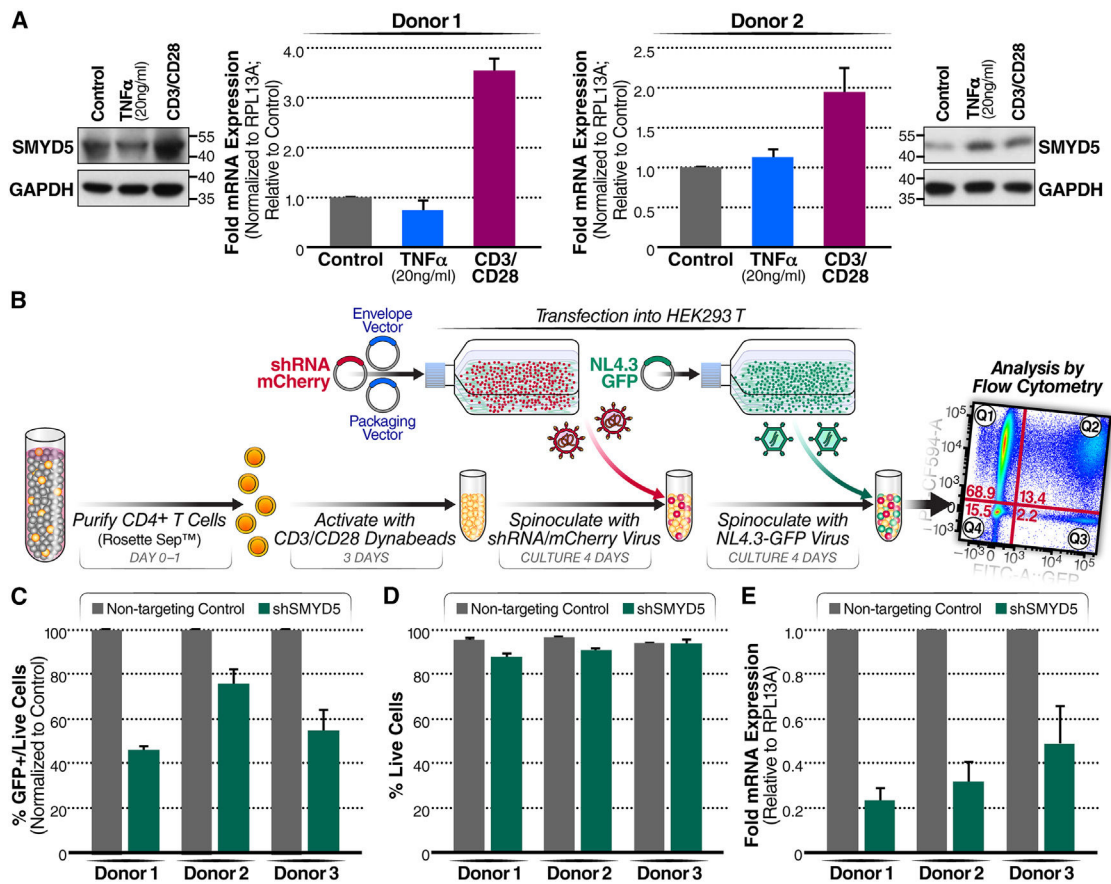


**Figure 2. SMYD5 is expressed and upregulated upon activation in primary CD4<sup>+</sup> T cells, and its knockdown inhibits HIV-1 expression**

(A) SMYD5 protein and mRNA expression in CD4<sup>+</sup> T cells from the blood of two independent human donors. The cells were treated with 20 ng/mL TNF- $\alpha$  or  $\alpha$ CD3/CD28 Dynabeads (1 bead per 2 cells) for 24 h, then lysed in FLAG immunoprecipitation (IP) buffer for western blot analysis or in RLT<sup>+</sup> lysis buffer to isolate mRNA (QIAGEN). RNA levels were analyzed by qRT-PCR and normalized to RPL13A RNA. The average (mean  $\pm$  SEM) from triplicate experiments performed with two different donors is shown.

(B) shRNA-mediated knockdown of SMYD5 in CD4<sup>+</sup> T cells. Shown is a schematic of the workflow. Primary CD4<sup>+</sup> T cells isolated from uninfected blood donors were activated with  $\alpha$ CD3/CD28 Dynabeads for 3 days, infected first with lentiviral particles encoding shRNA against SMYD5 or a non-targeting control, and second with a GFP-tagged reporter virus in the background of HIV<sub>NL4-3</sub>.

(C–E) Impact of non-targeting or SMYD5-targeting shRNAs on the percentage of HIV-1 expressing (GFP<sup>+</sup>) cells (C), the percentage of live cells as measured by forward scatter analysis and viability stain (D), and the level of SMYD5 mRNA as determined by RT-PCR normalized to RPL13A mRNA (E) among activated CD4<sup>+</sup> T cells from three independent donors. The average (mean  $\pm$  SEM) from triplicate experiments performed with three different donors is shown.

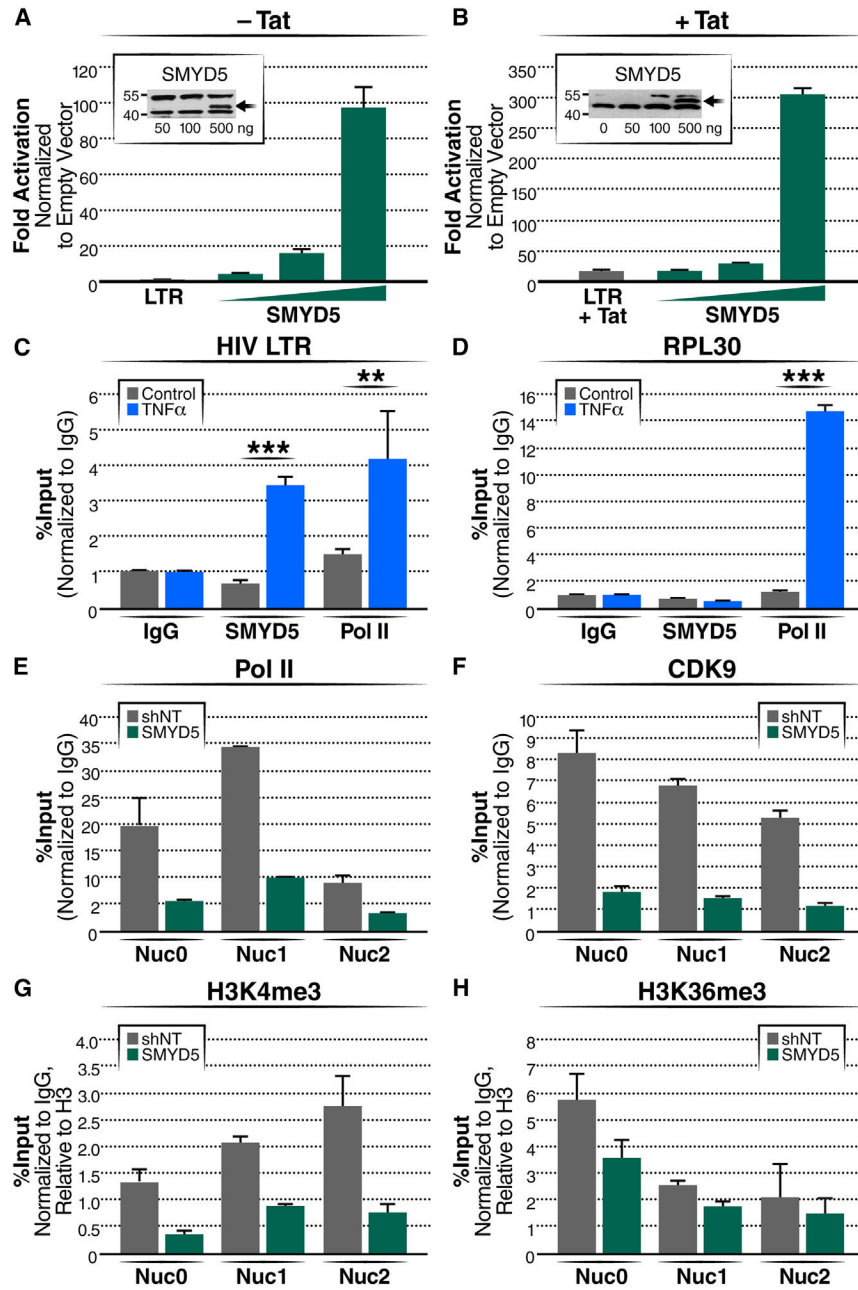


**Figure 3. SMYD5 is recruited to the HIV-1 LTR and activates HIV-1 transcription**

(A and B) Luciferase assays in HeLa cells transfected with an HIV-1 LTR luciferase construct and increasing amounts of an expression vector for SMYD5 (0, 5, 50, and 500 ng) in (A) the absence of Tat or (B) the presence of Tat. Expression of SMYD5 strongly activates the HIV-1 LTR and increases in the presence of Tat. Results of three biological replicates ( $\pm$ SEM) are shown. Insets show western blots, with arrows pointing to the SMYD5 band.

(C and D) ChIP assays with antibodies against SMYD5, RNA Pol II, and the IgG control at the HIV-1 LTR, followed by qPCR using primers specific for (C) the HIV-1 5' LTR or (D) the RPL30 control. Chromatin was prepared from J-Lat 5A8 cells treated with TNF- $\alpha$  to

stimulate the LTR or left untreated. The average of three independent experiments analyzed in triplicate  $\pm$  SEM is shown and compared with no-treatment control samples by ANOVA: \*\*p < 0.005, \*\*\*p < 0.001.

(E–H) ChIP assays with antibodies against RNA Pol II, CDK9, H3, H3K4me3, H3K36me3, and the IgG control at the HIV-1 LTR, followed by qPCR using primers specific for the HIV-1 LTR Nuc0, Nuc1, or Nuc2 regions. Chromatin was prepared from J-Lat A72 SMYD5 knockdown or non-targeting shRNA-expressing cells treated with TNF- $\alpha$  to stimulate the LTR. All ChIPs and qPCRs were repeated at least three times, and representative results of three technical replicates are shown.



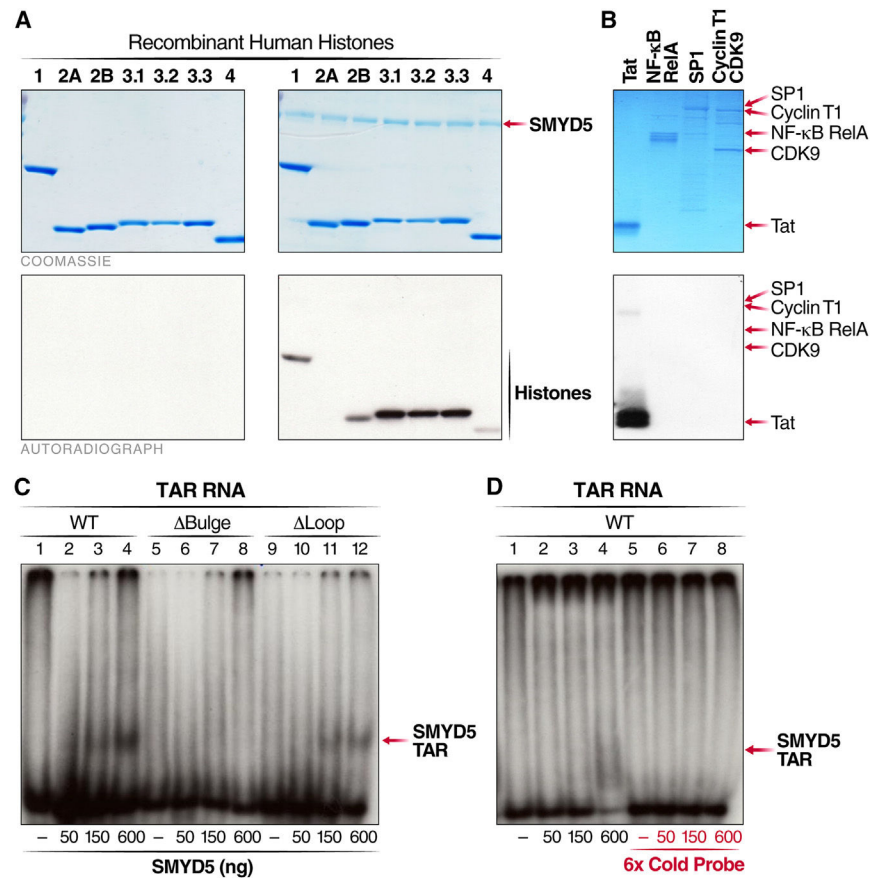


**Figure 4. SMYD5 methylates histones and Tat *in vitro* and binds TAR RNA**

(A and B) *In vitro* methylate recombinant histones (A) and synthetic Tat peptide (aa 1–72), recombinant NF- $\kappa$ B RelA, Sp1, Cyclin T1, or CDK9 incubated with recombinant full-length SMYD5 enzyme and radiolabeled H<sup>3</sup>-S-adenosyl-L-methionine (SAM). All *in vitro* methylation assays on isolated histones, Tat peptides, NF- $\kappa$ B, SP1, and pTEFb were repeated at least three times, and representative Coomassie staining (top) and corresponding autoradiographs (bottom) are shown.

(C) Gel shift assays of recombinant SMYD5 (0, 50, 150 and 600 ng) and radiolabeled wild-type (WT), bulge-mutant (ΔBulge), or loop-mutant (ΔLoop) TAR RNA probes.

(D) Gel shift assay with radiolabeled wild-type (WT) TAR RNA and increasing amounts of SMYD5 in the absence (left) and presence (right) of a 6× excess of non-radiolabeled TAR RNA. All EMSAs were repeated at least three times, and representative autoradiographs are shown.

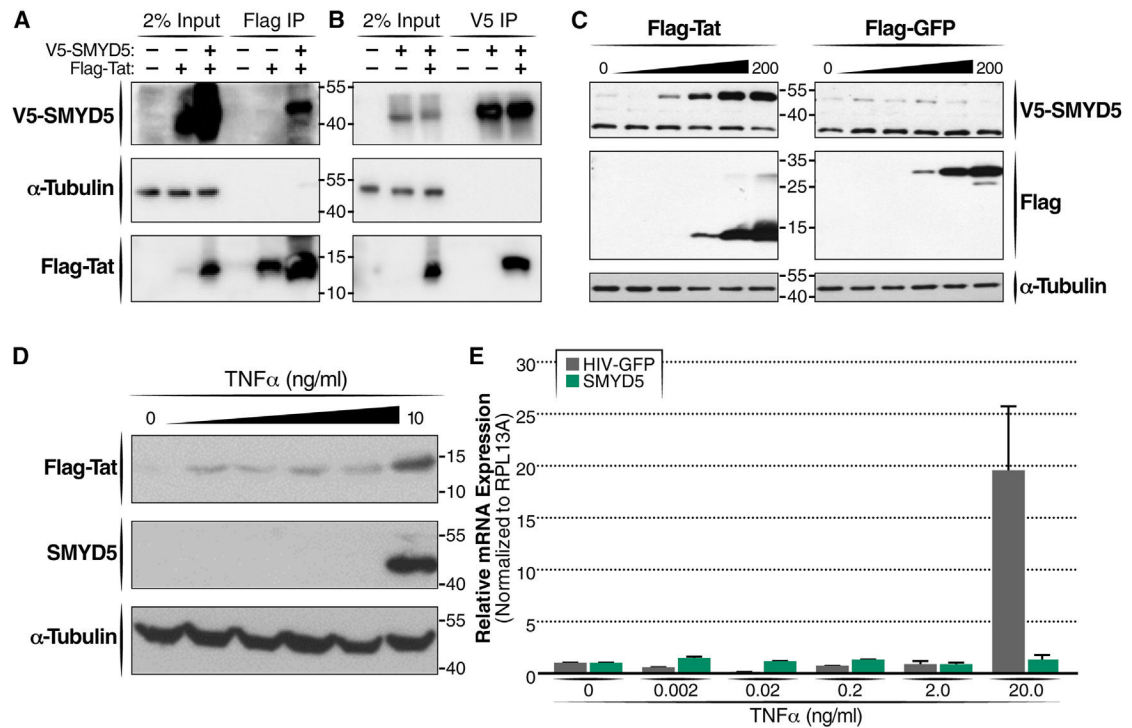


**Figure 5. Tat physically associates with SMYD5 and stabilizes SMYD5**

(A) SMYD5 co-immunoprecipitates with Tat. Cellular extracts from HEK293T cells expressing V5-SMYD5 or empty vector, alone or together with FLAG-Tat, were prepared 48 h after transfection and subjected to purification with anti-M2 FLAG affinity gel. The eluates were resolved by SDS-PAGE and subjected to western blotting.

(B) Tat co-immunoprecipitates with SMYD5. Cellular extracts from HEK293T cells expressing V5-SMYD5 or empty vector, alone or together with FLAG-Tat, were prepared 48 h after transfection and subjected to purification with anti-V5 affinity gel. The eluates were resolved by SDS-PAGE and subjected to western blotting.

(C) Tat increases SMYD5 protein expression. HEK293T cells were transfected with 500 ng V5-SMYD5 and 0–200 ng of FLAG-Tat or 0–200 ng FLAG-GFP plasmids. After 48 h, cells were lysed and subjected to western blot analysis.

(D and E) TNF- $\alpha$  increases SMYD5-Tat co-immunoprecipitation but not SMYD5 RNA production. J-Lat 5A8 cells were treated with increasing amounts of TNF- $\alpha$ . After 48 h, cells were lysed in FLAG-IP buffer and subjected to western blot analysis (C) or lysed in RLT<sup>+</sup> buffer to isolate mRNA (QIAGEN) (D). RNA levels were analyzed by qRT-PCR and normalized to RPL13A RNA. All IPs, western blots, and qPCRs were repeated at least three times. Representative results of IPs and western blots are shown. qPCR results of three biological replicates ( $\pm$ SEM) are shown.

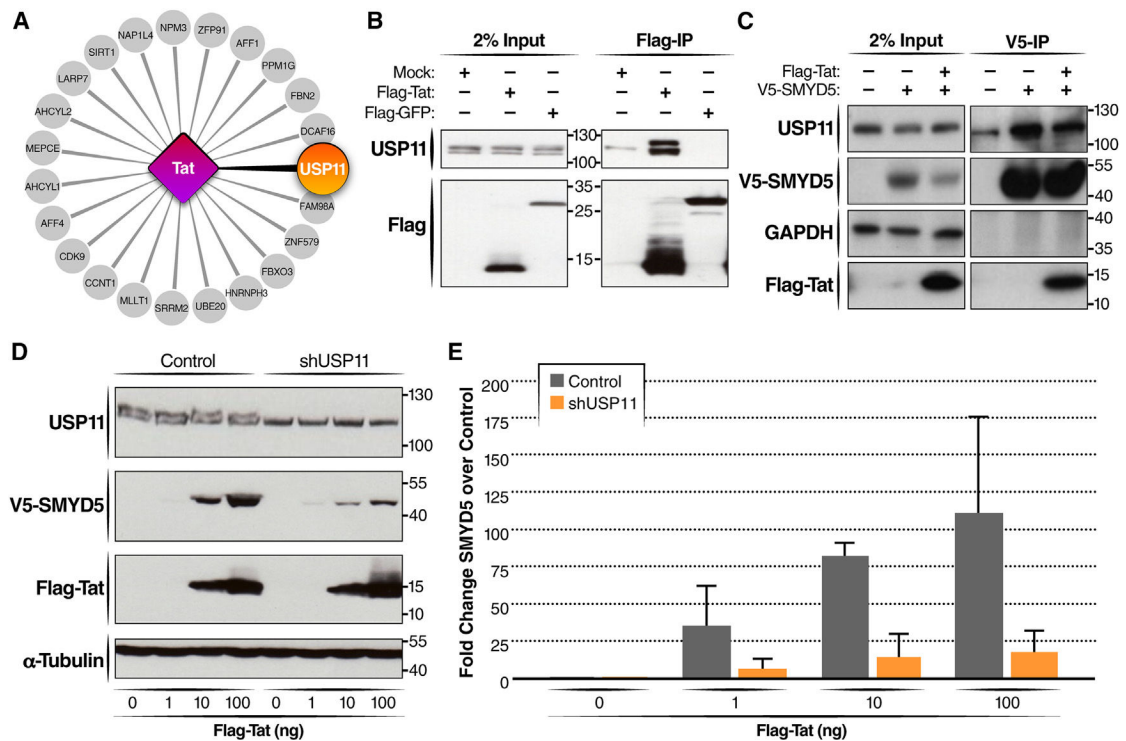


### Figure 6. SMYD5 and Tat interact with USP11

(A) Network representation of the interactions of HIV-1 Tat with human proteins,<sup>36</sup> highlighting USP11.

(B) Endogenous USP11 co-immunoprecipitates with FLAG-Tat. HEK293T cells were transfected with 200 ng of FLAG-Tat WT, FLAG-GFP, or empty vector. After 48 h cells were lysed in FLAG IP buffer and subjected to FLAG IP and Western blot analysis of endogenous USP11. Note that we consider the lower band in the blot nonspecific because it is not downregulated in (D).

(C) Tat and endogenous USP11 co-immunoprecipitate with V5-SMYD5. HEK293T cells were transfected with plasmids expressing V5-SMYD5 or empty vector, alone or together with FLAG-Tat. After 48 h, cells were lysed in FLAG IP buffer and subjected to V5 immunoprecipitation and western blot analysis. All IPs and western blots were repeated at least three times. Representative results of IPs and western blots are shown.

(D) USP11 knockdown inhibits Tat-mediated SMYD5 stabilization. HeLa cells were transduced with lentiviral vectors expressing shRNA targeting USP11 or a non-targeting control and selected by puromycin treatment. Successfully transduced cells were transfected with increasing amounts of Tat and, after 48 h, subjected to western blot analysis. Note that we consider the lower band in the blot nonspecific.

(E) Quantification of 3 independent experiments/western blots of SMYD5 bands in (D) by densitometric analyses using ImageJ. Each V5-SMYD5 band from shUSP11 was compared with its corresponding control-treated band (for example, 1 ng Tat control vs. 1 ng Tat shUSP11). Data are represented as means plus SEM.

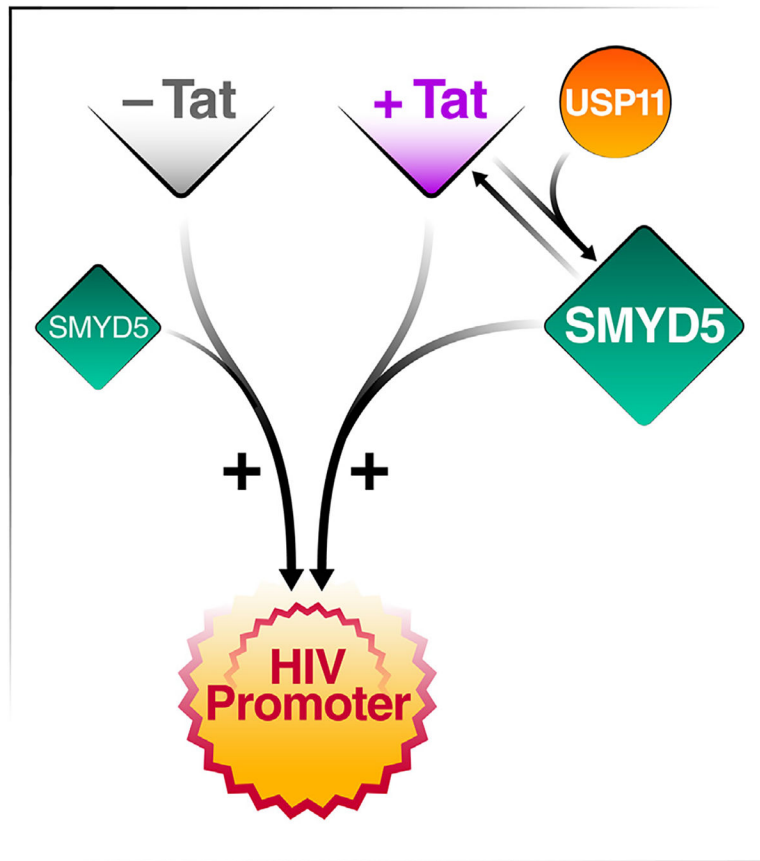


**Figure 7. Model of SMYD5's activator function at the HIV-1 LTR**

SMYD5 can activate the HIV-1 LTR alone through its intrinsic TAR RNA-binding capacity and in conjunction with Tat.

## KEY RESOURCES TABLE

REAGENT or RESOURCE	SOURCE	IDENTIFIER
Antibodies		
Alpha-Tubulin	Sigma-Aldrich	Cat# T6074; RRID: AB_477582; Clone 5-5-1-2; Lot# 0000089450
Alpha-Tubulin	Sigma-Aldrich	Cat# SAB3501071; RRID: AB_2713894
CD4-FITC	BioLegend	Cat# 357406; RRID: AB_2562357; Clone A161A1; Lot# B241850
CDK9	Cell Signaling	Cat# 2316S, Lot# 7
CDK9	Santa Cruz	Cat# sc-484, Lot#A0716; RRID: AB_2275986
FLAG	Sigma-Aldrich	Cat# F7425-2MG; RRID: AB_439687
GAPDH	Santa Cruz	Cat# sc-365062; RRID: AB_10847862; Lot# 1620
Histone H3	Active Motif	Cat # 39763; RRID: AB_2650522
Histone H3	Cell Signaling	Cat# 4499T, Lot# 9
Histone H3K4me3	Active Motif	Cat# 39915; RRID: AB_2687512
Histone H3K36me3	Cell Signaling	Cat# 4909T, Lot# 7
IgG Rabbit Isotype Control	Thermo Fisher Scientific	Cat# 10500C; RRID: AB_2532981
IgG-HRP Anti-Mouse	Rockland	Cat# 18-8817-33; RRID: AB_2610851; Clone eB144; Lot# 38282
IgG-HRP Anti-Rabbit	Rockland	Cat# 18-8816-33; RRID: AB_2610848; Clone eB182; Lot# 40107
RNA Polymerase II	Active Motif	Cat# 39097; RRID: AB_2732926; Clone 4H8; Lot# 24818020
RelA-NF-kB	Bethyl Laboratories	Cat# A301-824A; RRID: AB_1264341; Lot# A301-824A-2
SMYD5	Abcam	Cat# ab81419; RRID: AB_186119; Lot# 108176-1, 171198-1, 232795-1, 64744-4, 64744-7
SMYD5	Abcam	Cat# ab137622; Lot# GR109407-19
USP11	Bethyl Laboratories	Cat# A301-613A; RRID: AB_1211380; Lot# A301-613A-1, A301-613A-2
USP11 [EPR4346]	Abcam	Cat# ab109232; RRID: AB_10862711; Lot# GR3249106-5
Rabbit Polyclonal Anti-V5-Tag	Bethyl Laboratories	Cat# A190-120A; RRID: AB_67586; Lot# A190-120A-5
Rabbit Polyclonal Anti-V5-Tag	Abcam	Cat# ab15828; RRID: AB_443253; Lot# GR3198953-2
Anti-FLAG® M2 Affinity Gel	Sigma Aldrich	Cat# A2220; RRID: AB_10063035
V5-Tag Antibody Agarose	Sigma Aldrich	Cat# A7345-1ML; RRID: AB_10062721; Clone V5-10
Bacterial and virus strains		
MAX Efficiency™ DH5α Competent Cells	Thermo Fisher	Cat# 18258012
NEB® 10-beta Competent <i>E.coli</i>	New England Biolabs	Cat# C3019
One Shot™ Stbl-3™ Chemically Competent <i>E.coli</i>	Thermo Fisher	Cat# C737303
HIV-1 NL <sub>4-3</sub> -GFP	Kutsch et al. <sup>60</sup>	N/A

REAGENT or RESOURCE	SOURCE	IDENTIFIER
Biological samples		
Leukocyte Reduction Chamber from Trima Apheresis Collection	Vitalant Blood Donation, San Francisco	<a href="http://www.vitalant.org/">http://www.vitalant.org/</a>
Chemicals, peptides, and recombinant proteins		
CTP, [ $\alpha$ - <sup>32</sup> P]-800Ci/mmol 10mCi/ml, 250 $\mu$ Ci	Perkin Elmer	Cat# BLU008X250UC
Dynabeads® Human T-Activator CD3/CD28	Life Technologies	Cat# 11131D; Lot# 00979236
eBioscience™ Cell Stimulation Cocktail (500x)	Thermo Fisher Scientific	Cat# 00-4970-93; Lot# 2430455
Halt Protease & Phosphatase Inhibitor Cocktail	Thermo Fisher Scientific	Cat# 1861282
Surfact-Amps NP-40	Thermo Scientific	Cat# 28324
S-adenosylmethionine (SAM)	New England Biolabs	Cat# B9003S; Lot# 1221803, 10153874
Tumor Necrosis Factor- $\alpha$ , Human, Peprotech	Thermo Fisher Scientific	Cat# 300-01A; Lot# 021825L0621, 021825C1422
CDK9/Cyclin T1, Human, Recombinant	Thermo Fisher Scientific	Cat# PV4131; Lot# 1860128B
AMV Reverse Transcriptase	Promega	Cat# M5101
SYBR Green PCR Master Mix	Applied Biosystems	Cat# 4309155
X-tremeGENE 9 DNA Transfection Reagent	Roche	Cat# XTG9-RO
Histone H1, Human, Recombinant	New England Biolabs	Cat# M2501S; Lot# 0061508
Histone H2A, Human, Recombinant	New England Biolabs	Cat# M2502S; Lot# 0131508
Histone H2B, Human, Recombinant	New England Biolabs	Cat# M2505S; Lot# 0031508
Histone H3.1, Human, Recombinant	New England Biolabs	Cat# M2503S; Lot# 0041504
Histone H3.2, Human, Recombinant	New England Biolabs	Cat# M2506S; Lot# 0021504
Histone H3.3, Human, Recombinant	New England Biolabs	Cat# M2507S; Lot# 0021508
Histone H4, Human, Recombinant	New England Biolabs	Cat# M2504S; Lot# 0061508
HIV-1 Tat aa1-72, Recombinant	German Cancer Research Center Pagans et al. <sup>61</sup>	N/A
Micrococcal Nuclease	New England Biolabs	Cat# M0247S
NF $\kappa$ B p65, Human, Recombinant	Active Motif	Cat# 31102; Lot# 12312015
SMYD5 Human, Recombinant	Active Motif	Cat#31409; Lot# 06013001, 16314003
SP1, Human, Recombinant	Active Motif	Cat# 31136; Lot# 20011003
Critical commercial assays		
Dual-Luciferase® Reporter Assay System	Promega	Cat# E1910; Lot# 0000531188
Luciferase® Reporter Assay System	Promega	Cat# E1501; Lot# 0000486345
Direct-zol™ RNA Miniprep Kit	Zymo Research	Cat# 2052
GenElute™ Mammalian Genomic DNA Miniprep Kit	Sigma-Aldrich	Cat# G1N350
RNeasy Plus Mini Kit	Qiagen	Cat# 74136
eBioscience™ Fixable Viability Dye eFluor™ 780	Invitrogen	Cat# 65-0865-14; Lot# 2062571, 2450571
EasySepHuman CD4+ T Cell Isolation Kit	StemCell Technologies	Cat# 17952; Lot# 1000003548
RosetteSep Human CD4+ T Cell Enrichment Cocktail	StemCell Technologies	Cat# 15062; Lot# 18A86332, 19E101792
Riboprobe® <i>in vitro</i> Transcription Systems, T7	Promega	Cat# P1440; Lot# 0000429560, 0000470577
Experimental models: Cell lines		

REAGENT or RESOURCE	SOURCE	IDENTIFIER
HEK293T, Human, Female, Epithelial Kidney Cells	ATCC	CRL-3216 <sup>TM</sup>
HeLa, Human, Female, Epithelial Cervix Cells	ATCC	CCL-2 <sup>TM</sup>
J-Lat A2, Male, derived from Jurkat cells	Jordan et al. <sup>30</sup>	N/A
J-Lat A72 Male, derived from Jurkat cells	Jordan et al. <sup>30</sup>	N/A
J-Lat A5A8, Male, derived from Jurkat cells	Chan et al. <sup>27</sup>	N/A
Oligonucleotides		
For ChIP: Axin2 forward 5' GCCAGAGTC AAGCCAGTAGTC-3'	Rafati et al. <sup>62</sup>	N/A
For ChIP: Axin2 reverse: 5' TAGCCTAAT GTGGAGTGGATGTG-3'	Rafati et al. <sup>62</sup>	N/A
For ChIP: HIV LTR Nuc0 forward: 5' ATCTACCACACACAAGGCTAC-3'	Rafati et al. <sup>62</sup>	N/A
For ChIP: HIV LTR Nuc0 reverse: 5' GTACTAACTTGAAGCACCATCC-3'	Rafati et al. <sup>62</sup>	N/A
For ChIP: HIV LTR Nuc1 forward: 5' AGTGTGTGCCCGTCTGTTGT-3'	Boehm et al. <sup>20</sup>	N/A
For ChIP: HIV LTR Nuc1 reverse: 5' TTCGCTTTCAGGTCCCTGTT-3'	Boehm et al. <sup>20</sup>	N/A
For ChIP: HIV LTR Nuc2 forward: 5' GCGGAGGCTAGAAGGAGAGAG-3'	Rafati et al. <sup>62</sup>	N/A
For ChIP: HIV LTR Nuc2 reverse: 5' GCTCCCTGCTTGCCCATAC-3'	Rafati et al. <sup>62</sup>	N/A
For ChIP: RPL30 forward: 5' AAGGCAAAGCGAAATTGGTCA-3'	This manuscript	PrimerBank ID: 324021697c2; <a href="https://pga.mgh.harvard.edu/primerbank/">https://pga.mgh.harvard.edu/primerbank/</a>
For ChIP: RPL30 reverse: 5' TGCCACTGTAGTGATGGACAC-3'	This manuscript	PrimerBank ID: 324021697c2; <a href="https://pga.mgh.harvard.edu/primerbank/">https://pga.mgh.harvard.edu/primerbank/</a>
GFP qPCR Forward Primer: 5' ATGGTGAGCAAGGGCGAGGAG-3'	Drenan et al. <sup>63</sup>	N/A
GFP qPCR Reverse Primer: 5' GTGGTGCAGATGAACTTCAG-3'	This manuscript	N/A
SMYD5 qPCR Forward Primer: AATGCACTTTATCGCTACCGAG	This manuscript	PrimerBank ID: 154689857b3; <a href="https://pga.mgh.harvard.edu/primerbank/">https://pga.mgh.harvard.edu/primerbank/</a>
SMYD5 qPCR Reverse Primer: CTGCCAACCGACATTCTGC	This manuscript	PrimerBank ID: 154689857b3; <a href="https://pga.mgh.harvard.edu/primerbank/">https://pga.mgh.harvard.edu/primerbank/</a>
USP11 qPCR Forward Primer: AATGCACTTTATCGCTACCGAG	This manuscript	PrimerBank ID: 75992939c1; <a href="https://pga.mgh.harvard.edu/primerbank/">https://pga.mgh.harvard.edu/primerbank/</a>
USP11 qPCR Reverse Primer: CTGCCAACCGACATTCTGC	This manuscript	PrimerBank ID: 75992939c1; <a href="https://pga.mgh.harvard.edu/primerbank/">https://pga.mgh.harvard.edu/primerbank/</a>
RPL13A qPCR Forward Primer: GCCCTACGACAAGAAAAAGCG	This manuscript	PrimerBank ID: 14591905c2; <a href="https://pga.mgh.harvard.edu/primerbank/">https://pga.mgh.harvard.edu/primerbank/</a>
RPL13A qPCR Reverse Primer: TACTTCCAGCCAACCTCGTGA	This manuscript	PrimerBank ID: 14591905c2; <a href="https://pga.mgh.harvard.edu/primerbank/">https://pga.mgh.harvard.edu/primerbank/</a>
HIV-1 NL <sub>4-3</sub> 5' TR PCR forward primer: 5'-CTACCACACACAAGGCTACT-3'	Zhuang et al. <sup>64</sup>	N/A
HIV-1 NL <sub>4-3</sub> 5' TR PCR reverse primer: 5'-CTCGACCCATCTCTCCTT-3'	Zhuang et al. <sup>64</sup>	N/A
HIV-1 NL <sub>4-3</sub> gag PCR forward primer: 5' -TAGTAGAAGAGAAGGCTTTCAGC-3'	Zhuang et al. <sup>64</sup>	N/A
HIV-1 NL <sub>4-3</sub> gag PCR reverse primer: 5' -GTCCTTCTTTCACATTT CC-3'	Zhuang et al. <sup>64</sup>	N/A

REAGENT or RESOURCE	SOURCE	IDENTIFIER
HIV-1 NL <sub>4-3</sub> <i>pol</i> PCR forward primer: 5'-GCAAGGCCAATGGACATATCAA-3'	Zhuang et al. <sup>64</sup>	N/A
HIV-1 NL <sub>4-3</sub> <i>pol</i> PCR reverse primer: 5'-CTACAGTCTACTTGTCCATGCA-3'	Zhuang et al. <sup>64</sup>	N/A
HIV-1 NL <sub>4-3</sub> <i>vpr</i> PCR forward primer: 5'-GGAAAGGACCAGCAAAGCT-3'	Zhuang et al. <sup>64</sup>	N/A
HIV-1 NL <sub>4-3</sub> <i>vpr</i> PCR reverse primer: 5'-CTGCTATGTGCGACACCCAAT-3'	Zhuang et al. <sup>64</sup>	N/A
Recombinant DNA		
Lentiviral Packaging Construct pCMVdelta R8.91	Naldini et al. <sup>65</sup>	N/A
VSV-G Glycoprotein-expressing Vector	Naldini et al. <sup>65</sup>	N/A
SMYD5 #1 TRC Human shRNA	Thermo Scientific	TRCN0000155095
SMYD5 #2 TRC Human shRNA	Thermo Scientific	TRCN0000156306
USP11 #1 TRC Human shRNA	Thermo Scientific	TRCN0000007358
USP11 #1 TRC Human shRNA	Thermo Scientific	TRCN0000315152
Non-targeting Human shRNA	Millipore Sigma	SHC002
pLKO.1 mCherry	Addgene	Cat# 128073, RRID: Addgene_120873
pLenti6.2/V5-SMYD3	DNASU	Cat# HsCD00329555
pLX304/V5-WHSC1L1 (V5-NSD3)	DNASU	Cat# HsCD00444436
pLenti6.2/V5-SMYD5	DNASU	Cat# HsCD00329698
pDONR221-SMYD5	DNASU	Cat# HsCD00829682
Flag-HIV-1 Tat	Pagans et al. <sup>66</sup>	N/A
Flag-HA-GFP	Sowa ME et al. <sup>67</sup>	Addgene plasmid # 22612; <a href="http://n2t.net/addgene:22612">http://n2t.net/addgene:22612</a> ; RRID:Addgene_22612
Empty pEF-BOS	Pagans et al. <sup>66</sup>	N/A
HIV-1 TAR WT	Kaehlke et al. <sup>35</sup>	N/A
HIV-1 TAR Bulge	Kaehlke et al. <sup>35</sup>	N/A
HIV-1 TAR Loop	Kaehlke et al. <sup>35</sup>	N/A
EF1 $\alpha$ -Renilla	Kasler et al. <sup>68</sup>	N/A
HIV-1-LTR Luciferase	Van Lint et al. <sup>69</sup>	N/A
Software and algorithms		
AlphaView – AlphaImagerHP 3.5.0.927	ProteinSimple	<a href="https://www.proteinsimple.com/resources">https://www.proteinsimple.com/resources</a>
FlowJo 9.9-10.8	Tree Star	<a href="https://www.flowjo.com/">https://www.flowjo.com/</a>
ImageJ	NIH	<a href="https://imagej.nih.gov/ij/">https://imagej.nih.gov/ij/</a>
Prism8	GraphPad	<a href="https://www.graphpad.com/scientific-software/prism/">https://www.graphpad.com/scientific-software/prism/</a>
SDS 2.4 software	Applied Biosystems	<a href="http://home.appliedbiosystems.com">http://home.appliedbiosystems.com</a>
SoftMax® Pro 4.7.1 – 6.5.1	Molecular Devices	<a href="https://www.moleculardevices.com/products/microplate-readers/acquisition-and-analysis-software/softmax-pro-software#gref">https://www.moleculardevices.com/products/microplate-readers/acquisition-and-analysis-software/softmax-pro-software#gref</a>